BARC/2004/E/009

BARC/2004/E/009

THERMODYNAMICS AND PHASE DIAGRAMS OF THE PLUTONIUM-URANIUM, URANIUM-ZIRCONIUM, PLUTONIUM-ZIRCONIUM AND PLUTONIUM-URANIUM-ZIRCONIUM SYSTEMS

by

R. Agarwal and V. Venugopal
Fuel Chemistry Division

भारत सरकार
Government of India
भाभा परमाणु अनुसंधान केंद्र
Bhabha Atomic Research Centre
मुंबई Mumbai - 400 085, भारत India

2004

BIBLIOGRAPHIC DESCRIPTION SHEET FOR TECHNICAL REPORT
(as per IS : 9400 - 1980)

01	*Security classification :*	Unclassified
02	*Distribution :*	External
03	*Report status :*	New
04	*Series :*	BARC External
05	*Report type :*	Technical Report
06	*Report No. :*	BARC/2004/E/009
07	*Part No. or Volume No. :*	
08	*Contract No. :*	
10	*Title and subtitle :*	Thermodynamics and phase diagrams of the plutonium-uranium, uranium-zirconium, plutonium-zirconium and plutonium-uranium-zirconium systems
11	*Collation :*	65 p., 19 figs., 13 tabs.
13	*Project No. :*	
20	*Personal author(s) :*	R. Agarwal; V. Venugopal
21	*Affiliation of author(s) :*	Fuel Chemistry Division, Bhabha Atomic Research Centre, Mumbai
22	*Corporate author(s) :*	Bhabha Atomic Research Centre, Mumbai - 400 085
23	*Originating unit :*	Fuel Chemistry Division BARC, Mumbai
24	*Sponsor(s) Name :*	Department of Atomic Energy
	Type :	Government

Contd...

30	*Date of submission :*	April 2004
31	*Publication/Issue date :*	May 2004
40	*Publisher/Distributor :*	Head, Library and Information Services Division, Bhabha Atomic Research Centre, Mumbai
42	*Form of distribution :*	Hard copy
50	*Language of text :*	English
51	*Language of summary :*	English
52	*No. of references :*	95 refs.
53	*Gives data on :*	

60 *Abstract :*

Thermodynamic and phase diagram data reported in literature for the binaries, Pu-U, Pu-Zr and U-Zr, were compiled and optimised to calculate Gibbs energies of all the binary phases of these systems. Lukas program was used to carry out these optimisations, where, thermodynamic and phase diagram data of all the binary phases of a binary system were optimised simultaneously. Gibbs energy sets thus calculated were used to compare our results with the experimental and calculated phase diagram and thermodynamic data reported in the literature. The Gibbs energies of the binary systems were then compiled together to define Pu-U-Zr ternary system.

70	*Keywords/Descriptors :*	ALLOY NUCLEAR FUELS; FBR TYPE REACTORS; PLUTONIUM; URANIUM; ZIRCONIUM; BURNUP; BINARY ALLOY SYSTEMS; TERNARY ALLOY SYSTEMS; PHASE DIAGRAMS; FREE ENTHALPY; DATA ANALYSIS; PHASE STUDIES
71	*INIS Subject Category :*	S11
99	*Supplementary elements :*	

सारांश

द्विनात्विक निकाय, Pu-U, Pu-Zr और U-Zr, के लिए साहित्य में दिए गए उष्मगतिकि और आवस्था - रेखाचित्र के व्यौरे का संकलन करके उनका विश्लेषण किया गया। गणना के द्वारा इन सब निकायों की विभिन्न अवस्थायों के गिब्स-उर्जा समुह को निकाला गया। लूकाज प्रोग्राम के द्वारा की गइ इस गणना में किसी एक द्विनात्विक निकाय के सब रूपों के लिए दिए गए सब तथ्यों का एक साथ प्रयोग करके गिब्स-उर्जा के समुह को परिभाषित किया गया। इस समुह के प्रयोग से निकाले गए उष्मगतिकि और आवस्था - रेखाचित्र के परिणामों की तुलना साहित्य में दिए गए नतीजों से किया गया। इन तीनों द्विनात्विक निकायों के गिब्स-उर्जा समुहों को एकत्रित करके Pu-U-Zr त्रिनात्विक निकाय की रचना की गई है।

ABSTRACT

Thermodynamic and phase diagram data reported in literature for the binaries, Pu-U, Pu-Zr and U-Zr, were compiled and optimised to calculate Gibbs energies of all the binary phases of these systems. Lukas program was used to carry out these optimisations, where, thermodynamic and phase diagram data of all the binary phases of a binary system are optimised simultaneously. Gibbs energy sets thus calculated were used to compare our results with the experimental and calculated phase diagram and thermodynamic results reported in the literature. The Gibbs energies of the binary systems were then compiled together to define Pu-U-Zr ternary system.

Thermodynamics and phase diagrams of the plutonium-uranium, uranium-zirconium, plutonium-zirconium and plutonium-uranium-zirconium systems

R. Agarwal and V. Venugopal
Fuel Chemistry Division, Bhabha Atomic Research Centre, Mumbai-400085, India

1. Introduction

Early fast nuclear reactors (EBR, EBR-II, FERMI, DFR etc.) used metallic fuels due to many advantages of metallic fuels over ceramic fuels, e.g., high density, high linear and specific power, high breeding ratios, higher thermal conductivity, reduced hardware a fabrication costs due to larger diameter fuel elements, and easy fabricability. However, due to its low solidus temperature, high swelling rate during burn up and high smearing density (85 to 100%), this fuel was later abandoned in favour of ceramic fuels. There is again an increased interest in metallic fuel for advanced fast breeder reactors. These metallic fuels have overcome the two main drawbacks of U-Pu metallic fuels. Advance metallic fuels are alloys with high melting metals, which increase the solidus temperature and reduce smearing density. Integrated Fast Reactor (IFR) concept developed by Argonne National Laboratory, uses an alloy with 70 wt%U-20%Pu-10%Zr [1,2]. It attained a burn up as high as 20 at.% [3]. To be able to predict the fuel behaviour at various composition and temperature ranges, critical assessment of the available thermodynamic and phase diagram data is very important. Present work was undertaken to compile, assess and optimize all the experimental information on thermodynamic and phase equilibrium behaviour of the ternary system and its binary systems.

2. Calculation methods and results

To carry out optimization calculations, Gibbs energies of the constituent elements were defined as a function of temperature for all their allotropes. The Gibbs energy values of the elements were expressed as a function of temperature using the following SGTE description:

$$G(T)-H^{ref}(298.15\ K) = A + B\times T + C\times T\times \ln T + D\times T^2 + E/T + F\times T^3, \quad (1)$$

where, G(T) is the Gibbs energy of an element at temperature T(K) and $H^{ref}(298.15\ K)$ is the enthalpy of the stable reference phase of that element at 298.15 K. Elemental Gibbs energy values were taken from literature.

To calculate phase diagrams and thermodynamic properties of a binary system A-B, all the available experimental data on thermodynamic properties and phase equilibrium behaviour of the binary systems were compiled and critically assessed. Both thermodynamic and phase diagram data was optimised simultaneously, using Lukas program [4,5], to get Gibbs energies of formation of binary phases. The Gibbs energies of formation of stoichiometric compounds were defined as a function of temperature, expressed by the following polynomial:

$$\Delta G^f = A + B\times T + C\times T\times \ln T + D\times T^2 + E/T + F\times T^3. \quad (2)$$

Whereas, Redlich-Kister polynomials [6] were used for defining excess Gibbs energies of non-stoichiometric compounds and solution phases.

$$G^{ex} = X_A X_B \sum_{i=0,n} K_{i+1}(X_A - X_B)^i , \quad (3)$$

where, x_A and x_B are mole fractions of components A and B, respectively and K_{i+1} is a function of temperature as follows:

$$K_{i+1} = A_{i+1}+B_{i+1}\times T+C_{i+1}\times T\times \ln T+D_{i+1}\times T^2. \quad (4)$$

Therefore, Gibbs energies of formation of solution phases and non-stoichiometric phases can be expressed as:

$$\Delta G_f^o = RT(X_A \ln X_A + X_B \ln X_B) + X_A X_B \sum_{i=0,n} K_{i+1}(X_A - X_B)^i , \quad (5)$$

Once all the binary systems Pu-U, Pu-Zr and U-Zr were appropriately defined, Gibbs energies of formation of the ternary phases of Pu-U-Zr system were calculated. Excess Gibbs energies of formation of the ternary phases were calculated based on available experimental data on the ternary system and optimised Gibbs energy values of the binary phases. In the absence of any experimental data for ternary phases, ideal solution of mixing of binary phases was assumed. The ternary phases were either pure binary phases or solutions of binary phases. No new ternary intermetallic compound is known to be formed in Pu-U-Zr system.

In the following sections each binary system is discussed separately and at the end the optimised Gibbs energy equations of binary phases are combined to define ternary system, Pu-U-Zr.

2.1. Plutonium-uranium

To calculate Gibbs energies of the binary phases of Pu-U system, Gibbs energies of all the allotropes of plutonium and uranium were taken as a function of temperature. Plutonium has six solid state allotropes and one liquid phase: primitive monoclinic plutonium(α), body-centred monoclinic plutonium(β), face-centred orthorhombic plutonium(γ), face-centred cubic plutonium(δ), face-centred tetragonal plutonium(δ'), body-centred cubic plutonium(ε) and liquid plutonium(l). Uranium metal has three solid state allotropes and one liquid phase: C-centred orthorhombic uranium(α), primitive tetragonal uranium(β), body-centred cubic uranium(γ) and uranium(l).

The Gibbs energy of plutonium(α) used in present calculations [7] is:

$$G^o_{Pu(\alpha)}\text{ (J/mol) (298.15 to 400 K)} = -7.3963\times10^3+80.3014\times T-18.126\times T\times \ln(T) - 2.24\times10^{-2}\times T^2,$$

$$\text{(for 400 to 944 K)} = -1.6606\times10^4+2.3679\times10^2\times T-42.42\times T\times \ln(T) - 1.34\times10^{-3}\times T^2+5.79\times10^5/T+2.63\times10^{-7}\times T^3,$$

$$(T>944\ K) \qquad = -1.4462\times10^{4}+2.3296\times10^{2}\times T-42.248\times T\times\ln(T). \qquad (6)$$

The Gibbs energy of uranium(α) [7] was defined as follows:

$$G^{0}_{U(\alpha)}\ (J/mol)\ (298.15\ to\ 955\ K) = -8.407734\times10^{3}+1.30947151\times10^{2}\times T-26.9182\times T\times\ln(T) +1.25156\times10^{-3}\times T^{2}+3.8568\times10^{4}/T-4.42605\times10^{-6}\times T^{3},$$

$$(for\ T>955\ K) \qquad = -2.25218\times10^{4}+2.92113093\times10^{2}\times T-48.66\times T\times\ln(T), \qquad (7)$$

The Gibbs energies of other allotropes of plutonium and uranium were calculated from the Gibbs energies of respective alpha phases, using enthalpies and temperatures of transitions of the allotropes. The Gibbs energies of transitions for plutonium and uranium allotropes were taken from Leibowitz et al.[8] and are given in tables 1 and 2, respectively. To calculate Gibbs energies of the binary intermetallic compounds of plutonium-uranium system, η and ζ, Gibbs energies of hypothetical Pu(η), Pu(ζ), U(η) and U(ζ) elementary phases were required. These estimated values were taken from Leibowitz et al.[8]. For estimation of Gibbs energies of hypothetical elementary phases, appropriate binary phase boundaries were extrapolated to the pure elements, which gave hypothetical transition temperatures.

The important features of Pu-U binary alloy system are: (i) presence of two intermetallic compounds, a high temperature tetragonal phase eta (η) and a low temperature cubic phase that is stable at room temperature, zeta (ζ), both showing a wide non-stoichiometry, (ii) negligible solubility of uranium in most of the plutonium allotropes, whereas, all allotropes of uranium dissolve considerable amounts of plutonium, (iii) a BCC binary phase of Pu-U system, relevant to nuclear fuel, i.e., a solid-solution of Pu(ε) and U(γ). This phase is stable over the complete composition range. Except for the composition range with high uranium content, this phase is stable over a limited temperature range, (iv) liquidus-solidus curves of this system show a minimum on plutonium side.

Experimental data available on Pu-U system is very limited, especially at low temperatures. Moreover, the available experimental data shows discrepancies. All the important experimental and calculation works related to phase equilibria or thermodynamic studies of this system are listed in table 3.

2.1.1. Solubility of uranium in plutonium allotropes

Bochvar et al. [9] have compiled their work on many plutonium alloys. They have not given any description of the techniques used by them in those analysis which made it difficult for the present authors to assess the reliability of their work. They have reported less than 2 at.% uranium solubility in (αPu). But they stated that (βPu) tends to get stabilised at room temperatures in the binary system, therefore, alloys containing up to 25 at.% uranium are stable in (βPu)+ζ phase field at room temperature even with very slow cooling rates. Bochvar et al. have reported a maximum solubility of 17 at.% uranium in β-plutonium. Ellinger et al.[10] have constructed a plutonium rich phase diagram (up 5 at.% uranium) using high temperature diffractometer and dilatometer. They indicated negligible solubility of uranium in alpha-plutonium and (βPu) dissolves maximum amount of uranium (~ 2 at.% uranium) at 553 K, the peritectoid equilibrium temperature for the reaction: (γPu)+η↔(βPu). At this

temperature, (γPu) dissolves up to 0.8 at.% uranium. The solubility limits of uranium in (δPu) changes from 0.2 at.% uranium at the peritectoid temperature, 593 K, for the reaction, (γPu)↔(δPu)+η, to 0.3 at.% uranium at the peritectoid temperature, 715 K, for the reaction, (δPu)+η↔(δ'Pu). The plutonium allotrope, Pu(δ') dissolves up to 1.3 at.% uranium at 728 K. Waldron [11] has reported phase diagram studies of plutonium alloys undertaken by UKAEA. Various techniques like, thermal analysis, dilatometry, metallography, and X-ray crystallography were employed for those studies. In the report, Waldron [11] has indicated that the work at Harwell confirmed with the work reported from Los Alamos except for some difference in the homogeneity range of the BCC solid-solution, which will be discussed later. A Pu-U phase diagram, with an inset of plutonium rich partial phase diagram given by Schonfeld [12], based on the data obtained at the Los Alamos Scientific Laboratory, using optical micrography, X-ray metallography, thermal analysis, and dilatometry, is also identical to the one given by Ellinger et al. [10]. As discussed in a publication by Elliott and Larson [13], based on X-ray diffraction and dilatometric results, Pu(δ') dissolves appreciable amounts of a few elements like titanium, thorium and uranium, which stabilises (δ'Pu) to the temperatures lower than the transition temperature of pure plutonium, Pu(δ') → Pu(δ). Otherwise, most of the general impurities found in plutonium tend to destabilise this allotrope compared to Pu(δ) and Pu(ε).

During assessment of Pu-U phase diagram, Peterson and Foltyn [14] have accepted solubility limits of uranium in plutonium allotropes given by Ellinger et al. [10]. Leibowitz et al. [8] have also used these values for their optimization calculations. However, they faced some problem in calculating the change in solubility limits of uranium in (γPu) and (δPu) with change in temperature. Therefore, they have assumed uranium solubility in these two allotropes to be independent of temperature. For present optimization calculations, Ellinger et al. values of solubility limits were used and Gibbs energies of dissolution of uranium in all the allotropes of plutonium were assumed to be independent of temperature.

2.1.2. Solubility of plutonium in uranium allotropes

Berndt [15] determined plutonium solubility in α-uranium by Debye-Scherrer method and found 15 at.% plutonium solubility in α-uranium at 673 K. By thermal analysis, Ellinger et al. [10] indicated that by dissolution of plutonium, transition temperature of α-uranium to β-uranium is lowered from 941 K, for pure element, to 833 K, the temperature of eutectoid reaction (βU)↔(αU)+ζ. At this temperature α-uranium dissolves about 15 at.% plutonium, but indicates a small temperature dependence below this temperature, reaching about 11 at.% plutonium at 523 K. In the phase diagram given by Waldron [11] the solubility at 673 K is placed at 14 at.% plutonium. Bochvar et al. [9] have shown a maximum solubility of about 17 at.% plutonium in α-uranium in their phase diagram. But no experimental details were given in their publication, therefore, their data was not considered for optimisation.

Beta-uranium can dissolve more plutonium than alpha-uranium. According to Ellinger et al., maximum solubility of plutonium in beta-uranium is 20 at.% at 973 K. Below this temperature it decreases to about 18 at.% plutonium at 833 K, where it decomposes eutectoidally into (αU) and ζ (zeta) phases. Ellinger et al. also mentioned that the (βU) phase containing at least 10 at.% plutonium

can be retained at room temperature by water quenching. They determined the lattice constants of the tetragonal (βU) containing 15 at.% plutonium as a=10.61 and c=5.605 Å at room temperature and reported a calculated density of 18.78 g/cm^3. The phase diagram given by Bochvar et al.[9] gives a maximum solubility of about 33 at.% plutonium at 973 K, the peritectoid temperature of η↔(βU)+(ε-Pu,γ-U) equilibrium. But as mentioned earlier, they did not give any details of their experimental techniques, and their solubility limits of plutonium in uranium were found to be higher than other reported values. Therefore, their data was not considered for present calculation. In fact Schonfeld [12] has reported that Bochvar et al had later agreed that the solubility limits of plutonium in uranium should be close to the values given by Ellinger et al. [10]. Phase diagram given by Waldron [11] based on thermal analysis, X-ray analysis and dilatometry, are in general agreement with that of Ellinger et al. However, Waldron has shown that the solubility limit of plutonium in beta-uranium is almost independent of temperature and remains about 20 at.% plutonium from one eutectoid temperature 838 K, for the reaction (βU)↔(αU)+η, to another peritectoid temperature 978 K, for the reaction η↔(βU)+(ε-Pu,γ-U). Though Ellinger et al. have not given solubility of plutonium in (βU) involved in the peritectoid reaction η↔(βU)+(ε-Pu,γ-U), but reported the same peritectoid temperature, 978 K.

2.1.3. Intermetallic compounds of Pu-U system

The plutonium-uranium binary system has two intermetallic compounds ζ (zeta) and η (eta), which are stable over a wide composition range. The low temperature compound ζ, is stable at room temperature, whereas, η is a high temperature compound. Ellinger et al. [10] have reported formation of eta (η) by peritectoid reaction between beta-uranium and solid-solution phase (ε-Pu,γ-U) at approximately 70 at.% uranium and 978 K. They have assigned this phase a composition range of 2 at.% uranium at 593 K and 70 at.% uranium at 978 K. According to them, it decomposes eutectoidally by the reaction η↔(βPu)+ζ, at about 3 at.% uranium and 551 K. Based on X-ray analysis of the compound with 25 at.% uranium quenched from 773 K, they have reported η to be tetragonal with a unit cell containing 52 atoms and lattice parameters, a=10.57 Å and c=10.76 Å. Based on dilatometric results they gave the density of this compound as 17.3 g/cm^3. Ellinger et al. have given a table of diffraction data of η phase at room temperature, up to $\sin^2\theta$=0.3604. But they have mentioned that the solution of the powder pattern is highly uncertain as the X-ray powder pattern is very complex. Bochvar et al. [9] have also reported that η-intermetallic compound is stable over a wide composition range of 2 to 70 at.% uranium. Ellinger et al. [10] have determined the η↔η+(ε-Pu,γ-U) phase boundary by thermal analysis, dilatometry and X-ray diffraction. For present calculations, the phase boundary data was read from a small figure given by them.

Ellinger et al. have reported that the intermediate phase ζ is stable at room temperature. It is formed by peritectoid reaction, η+(βU)↔ζ, at about 72 at.% uranium and 863 K. With decrease in temperature it becomes stable with more plutonium content. The maximum solubility of plutonium in ζ is 75 at.% plutonium at 551 K The limit of the homogeneity range at its maximum width extends from about 25 at.% to about 74 at.% uranium. At room temperature its composition range of stability is between 33 at.% to 65 at.% uranium. According to Bochvar et al., ζ-compound is stable in the composition range 25 to 80 at.% uranium at room temperature and has a tetragonal lattice with lattice parameters a=10.73 Å, b=10.44 Å, with 56 atoms per unit cell. Whereas, Coffinberry [16] and Waldron [11] reported it to have cubic structure. Ellinger et al.[10] have reported that zeta (ζ) is tetragonal with axial ratio of unity at room temperature because high temperature X-ray indicates that ζ expands

anisotropically. However, they reported approximately 58 atoms per unit cell as calculated from the observed density of 18.8 g/cm^3. The X-ray pattern was indexed on the basis of primitive cubic unit cell and lattice constant is reported to decrease with increase in uranium content from a=10.692 Å at 35 at.% uranium to a=10.651 Å at 70 at.% uranium. They have listed a powder diffraction data of ζ, up to $\sin^2\theta$=0.3084.

The phase boundary of η/(η+ζ) was determined by Ellinger et al., mainly by metallographic analysis of heat treated and quenched alloys. They found that microstructures of some of the alloys quenched from η+ζ region were suitable for lineal and areal analysis. The phase boundary of ζ/(ζ+(αU)) was located by X-ray analysis of heat treated and quenched specimens. For present calculation these data were taken from the figure given by them. Okamoto et al. [17] also determined transition temperatures of various compositions of Pu-U alloys (11, 20, 42, 61, 70, 78 and 89 at.% U) by DTA. The compositions and the temperatures of all invariant reaction equilibria for this binary system selected by Peterson and Foltyn [14] were accepted for present calculations also.

2.1.4. Liquidus-solidus equilibrium

The minimum in the liquidus-solidus curves was observed by various workers. The liquidus curves given by Ellinger et al. [10] and in Mound Laboratory Report [18] agree well with each other. But solidus curves diverge by up to 40 K. Ellinger et al. have located liquidus and solidus by thermal analysis and microstructural analysis. They found a continuous liquid+(ε-Pu,γ-U) biphasic region broken by a minimum at about 12 at.% uranium and 883 K. This observation was confirmed by incipient melting in microstructural analysis at this composition and temperature. They have indicated that the liquidus could be defined appropriately over the most composition range by the thermal arrest obtained on cooling. Whereas, solidus could not be defined by thermal analysis except for the plutonium and uranium rich composition ends. Rosen et al. [19] have reported a minimum at 897 K and 9 at.% uranium. Wittenberg and Grove [20] have reported a minimum at 12-13 at.% uranium and 893 K by thermal analysis method. Wittenberg et al. [21] reported a minimum at 10 at.% uranium and 893 K, by using viscometer. Ellinger et al. [10] have concluded that solidus is a continuous curve and does not merge with (ε-Pu,γ-U)+η phase field because the alloys showed a clear thermal arrest to mark the upper boundary of (ε-Pu,γ-U)+η phase field. That could not have happened if the two phase fields had merged with each other. Chiotti et al. [22] have compiled all the available data on liquidus and solidus. In general, the solidus-liquidus curves given by Ellinger et al. [10], Bochvar et al.[9] and Waldron [11] agree reasonable well with each other.

2.1.5. Thermodynamics

Savage and Seibel [23] and later Savage [24] have reported heat content of Pu-U alloy with 90 at.% uranium in the temperature range 298.15 K to 1463 K, measured using an isothermal drop calorimeter. As can be seen from the phase diagram of this system that the Pu-U alloy with 90 at.% uranium is stable as (αU) at room temperature. But in the approximate temperature range 860 to 880 K, (αU) undergoes transition to (βU). At approximately 1030 K, (βU) changes into solid-solution, (ε-Pu,γ-U). Whereas, above ~1330 K this alloy is stable in liquid phase. Therefore, comparison of experimental enthalpy increment data of Savage had to be made with four different phases in the appropriate temperature ranges. Extrapolation of the heat content data of Savage and Seibel [23] for

liquid and solid solution, gave an enthalpy of fusion, 8.2 kJ/mol at 1323 K, for the alloy with 90 at.% U. According to Chiotti et al. [22], values of Savage and Seibel [23] do not give sensible heat capacity for allotropes of uranium.

McKenzie [25] has measured rates of evaporation of plutonium over very dilute solutions of plutonium in uranium at three different temperatures. Though the uncertainties of these measurements are large, the results indicated that the limiting value of activity coefficient of plutonium in liquid alloys is 1.00±0.25 in the temperature range 1813 to 2042 K. Even in present calculations best optimization results were obtained by assuming ideal solution behaviour for the Pu-U liquid phase.

2.1.6. Discussion

Based on SGTE expressions for Gibbs energies of all the unary allotropes as a function of temperature and all the above mentioned phase diagram and thermodynamic data of Pu-U, binary system, the excess Gibbs energies of the binary phases were calculated using Lukas program. These optimised excess Gibbs energies of binary phases are given in table 4. The Pu-U phase diagram calculated using these values is shown in figure 1. Phase boundary data reported in literature are also shown in this diagram for comparison. As can be seen, the optimised phase diagram compares well with the phase boundaries reported by Ellinger et al. [10]. These calculations were helpful in defining phase boundaries of η+(βU) phase field where no literature data was available. According to present calculations, this phase field is stable over a much narrower composition range compared to the one given by Peterson and Foltyn [14]. A partial phase diagram for plutonium rich region is given in figure 2. The phase boundaries of (Pu)/η, where (Pu) symbolises a solution of uranium in plutonium lattice, are in reasonably good agreement with Leibowitz et al. Whereas, it is at variance with Peterson and Foltyn. Solubility limits of uranium in (δPu) and (γPu) are lower in the partial phase diagram given by Peterson and Foltyn compared to phase diagram calculated using present optimized Gibbs energy values. On the other hand, at low temperatures, η phase is shown to be stable with higher plutonium content compared to present calculations. But these phase boundaries, with discrepancies, are given as dotted lines in the partial phase diagram given by Peterson and Foltyn, indicating uncertainty.

In uranium rich region, (βU)/η phase boundaries are different from both Leibowitz et al. and Peterson and Foltyn. To avoid a maximum in η/ζ equilibrium, in agreement with Pu-U phase diagram modelling by Leibowitz et al., and to retain Peritectoid equilibrium given by Ellinger et al. and Peterson and Foltyn, we had accepted a decrease in solubility limit of plutonium in U(β) with increase in temperature and a corresponding increase in the uranium content in η with increase in temperature. Therefore, effectively phase boundaries of (βU)/η equilibrium remained almost parallel as given by Leibowitz et al., but with reversed slopes. Ellinger et al. have defined the phase boundary of ζ phase in η/ζ equilibrium region reasonably well by thermal analysis. That is the only experimental data in this region, therefore, we gave full weightage to this data in present calculations, however, avoiding a maximum in η/ζ equilibrium given by Leibowitz et al. [8]. In the absence of any experimental data for the phase boundaries of (βU)/η equilibrium, it is difficult to assess the correct approach.

In table 5, invariant equilibrium temperatures and compositions of Pu-U binary system, calculated from the optimized Gibbs energy values during present calculations are given along with assessed values of Peterson and Foltyn [14] and experimental values of Leibowitz et al.[8]. Leibowitz

et al. have reported the equilibrium temperatures but not equilibrium composition., therefore, composition values were taken from the phase-diagrams given by them. As can be seen from the table 5, the invariant equilibrium calculated from present set of Gibbs energies are in better agreement with Peterson and Foltyn for uranium rich region, whereas, in plutonium rich region they are in good agreement with Leibowitz et al.

In present calculations, excess Gibbs energies of liquid phase was taken as zero, whereas, that of (ε-Pu,γ-U) was considered independent of temperature therefore, both the phases do not have any excess heat capacities. Hence, heat capacities of these phases of the Pu-U alloy with 90 at.% uranium should be sum total of the heat capacities of the stable phases of plutonium and uranium at respective temperatures in 1:9 ratio. In figure 3, calculated enthalpy increment values, in the temperature range 500 to 1500 K, of various binary phases of Pu-U system with 90 at.% uranium are compared with experimentally determined values reported by Savage and Seibel [23]. As can be seen that the values for binary phases, (αU) and (βU), agree very well with experimentally determined values. But experimental values are lower than calculated values in case of (ε-Pu,γ-U) and liquid. The enthalpy increment values reported by Savage and Seibel, for liquid phase, are much closer to the enthalpy increment data of pure plutonium liquid. Chiotti et al. [22] have discussed analysed enthalpy increment data of Savage and Seibel and concluded that the experimental data of Savage and Seibel does not give sensible heat capacity values for (βU) and (ε-Pu,γ-U). Extrapolation of least square fitted curves of enthalpy increment data given by Savage and Seibel for (ε-Pu,γ-U) and liquid phases gave an enthalpy of transition value 8.2 kJ/mol at 1323 K, whereas, Peterson and Foltyn have got it as 10.04 kJ/mol for the same data. In present calculations, the enthalpy of fusion of pure plutonium and uranium were taken as 2.82 kJ/mol at 913 K and 9.15 kJ/mol at 1406 K, respectively. On adding the enthalpies of fusion of pure elements, extrapolated to 1323 K, in the respective ratio for $Pu_{0.1}U_{0.9}$, we got 8.02 kJ/mol. This is in good agreement with that of Savage and Seibel but much lower than that of Peterson and Foltyn. This discrepancy may be attributed to the difference in the values used for enthalpy of fusion of elemental uranium (γ) at 1406 K. While, Peterson and Foltyn have used a value of 12.1 kJ/mol, in the present optimization calculations a value of 9.15 kJ/mol was taken, as given by Leibowitz et al. [26].

2.2. Plutonium-zirconium

To calculate the optimized Gibbs energies of this binary system, Gibbs energies of all the allotropes of plutonium and zirconium were needed. Allotropes of plutonium are already discussed in section 2.1 and their Gibbs energy values are given in equation (6) and table 1. Zirconium has two solid allotropes and one liquid phase namely, hexagonal close-packed zirconium(α), body-centred cubic zirconium(β) and zirconium(l).

The Gibbs energy of zirconium(α) allotrope used for present calculations is:

$$G^{o}_{Zr(\alpha)}\,(\text{J/mol})\ (T \geq 298.15\ \text{K}) = -7.06226\times10^{3}+1.1160405\times10^{2}\times T-21.966\times T\times\ln(T) -5.8\times10^{-3}\times T^{2}. \quad (8)$$

The Gibbs energies of other allotropes of zirconium were calculated from that of zirconium(α), using Gibbs energy of transitions from alpha phase to other phases as given in the table 6. The Gibbs energies of transitions for zirconium allotropes were taken from Ogawa and Iwai [27]. The Gibbs energies of the hypothetical allotropes of plutonium, Pu(ξ), Pu(θ), Pu(ι) and Pu(κ), and zirconium, Zr(ξ), Zr(θ), Zr(ι) and Zr(κ), were required for defining Pu-Zr binary system. The Gibbs energies of hypothetical 'ξ', 'θ' and 'ι' phases of plutonium and zirconium were assumed to be same as that of Pu(α) and Zr(α), respectively. Whereas, in case of 'κ' intermetallic compound, Gibbs energy of Zr(κ) was calculated by adding 846 J/mol in the value of Zr(α). As discussed in later parts of this publication, κ intermetallic compounds of Pu-Zr and U-Zr were found to be of very similar structure and completely soluble in each other in Pu-U-Zr ternary system. Therefore, Zr(κ) of Pu-Zr was assumed to have the same Gibbs energy as that of U-Zr system. However, the Gibbs energy of Pu(κ) was assumed to be same as that of Pu(α).

The main features of this system are: (i) presence of four intermetallic compounds, eta (ξ), theta (θ), iota (ι) and kappa (κ). The compounds, eta, theta and iota are plutonium rich compounds. Among these compounds, eta is stable over a narrow composition range [28], but in the absence of sufficient data, it was assumed to be a stoichiometric compound for present calculations. The compounds theta and iota are stable over a reasonably wide composition range. The compound, kappa is a zirconium rich non-stoichiometric compound. (ii) Addition of zirconium in plutonium increases the liquidus and solidus temperatures, which is a very useful aspect of the U-Pu-Zr metallic fuels. (iii) Pu(ε) and Zr(β) form a continuous BCC solid-solution, (ε-Pu,β-Zr), stable over the complete composition range and a wide temperature range. (iv) (δPu) dissolves considerable amount of uranium metal, however, solubility of zirconium in other allotropes of plutonium is very limited. Whereas, all allotropes of zirconium dissolve considerable amount of plutonium.

All the important publications reported in literature containing experimental data or assessment of phase equilibria or thermodynamic properties of this system are listed in table 7.

2.2.1. Solubility of zirconium in plutonium allotropes

Marples [29] has extensively investigated the plutonium-zirconium phase diagram from room temperature to 1573 K by thermal, dilatometric and X-ray analysis methods. He found that kinetics of the plutonium rich alloys, at low temperatures, is too slow for thermal analysis and dilatometry to be much reliable. Specially, (αPu)/(βPu) transformation is so sluggish that it can not be detected by thermal analysis, still he has marked the temperatures of thermal arrests in a phase diagram given in their publication. Based on X-ray diffraction work, he reported that (βPu) dissolves more zirconium than (αPu) and the transformation (βPu)↔(αPu) was depressed to the eutectoid temperature. He found that the (βPu) could be easily stabilized to room temperature even with slow cooling of the alloy. He reported some complications in X-ray diffraction analysis as well, because of the retention of (βPu) phase even in slowly cooled samples and complicated X-ray diffraction patterns of the equilibrium phases involved in this region, i.e., (αPu), (βPu) and the intermetallic compound. According to Marples, the intermetallic compound in equilibrium with (αPu) and (βPu) is θ, as presence of ξ compound was reported later by Ellinger and Land [28] and Taylor [30]. Marples determined the solubility of zirconium in (βPu) by the disappearing phase method. He observed a small change in $\sin^2\theta$ value with addition of zirconium in (αPu), but after addition of 1.5 to 2 at.% zirconium the $\sin^2\theta$

values remained constant. Based on these observations, Marples has reported approximate solubilities of zirconium in (αPu), (βPu) and (γPu) as 1.5, 7 and 3 at.% zirconium, respectively. Taylor did not determine actual solubility of zirconium in (αPu), (βPu) and (γPu) but suggested it to be lower than 1 at.% because the X-ray analysis of alloy with 1 at.% zirconium showed the presence of ξ compound. He found (αPu) with 0.25 at.% zirconium is single phase, therefore, according to him this may be the maximum solubility of zirconium in Pu(α). In the composition range 0.25 to ~2.5 at.% zirconium (αPu), (βPu) and (γPu) are in equilibrium with ξ compound. Based on X-ray diffraction and microstructural determination of the (γPu)/(γPu)+(δPu) and (γPu)/(γPu)+ξ phase boundaries, Ellinger and Land [28] have reported not more than 1.5 at.% zirconium solubility in (γPu) phase. They suggested a solubility of less than 1 at.% Zr for (βPu).

Suzuki et al. [31] carried out differential thermal analysis and X-ray diffraction analysis of Pu-Zr system with more than 50 at.% zirconium. According to them, the binary phase (δPu) dissolves at least 70 at.% zirconium at approximately 873 K. Waldron [11] also reported a solubility limit of 70 at.% zirconium in (δPu), though he did not mention the temperature. Later Ellinger and Land [28] carried out X-ray diffraction analysis of (δPu) alloys to determine zirconium solubility. They observed that (δPu) phase with minimum 4 at.% zirconium could be stabilised to room temperature only by quenching, whereas, (δPu) with more than 40 at.% zirconium was easily stabilised to room temperature. They have plotted lattice parameters of this phase as a function of composition. They observed that for the alloy composition 4 to 20 at.% zirconium, the reliability of the X-ray data was better than ±1 a% zirconium but with greater zirconium content alloys were difficult to homogenize and the reliability was not better than 2 at.% zirconium. Similarly, Marples [29] found that (δPu), FCC structure could be easily retained at room temperature except for highly plutonium rich compositions. Highly plutonium rich binary phase (δPu), containing more than 95 at.% plutonium, converts in lower temperature plutonium phases on lowering the temperature. Ellinger and Land [28] have given a plot of lattice parameters as a function of composition. In this plot, a marked inflection was observed at 20 at.% zirconium. From the mean lattice parameter for the (δPu) phase in (δPu)+(αZr) phase-field, treated at 873 K for 3 to 4 weeks, they have placed a solubility limit of 70 at.% (± 2at.%) zirconium at 894 K, the eutectoid temperature. They also found that the (δPu) solvus composition at (δPu)/(αZr) phase equilibrium was almost vertical as the solubility limit remains unchanged by subsequent treatments at 723 K and 573 K. Ellinger and Land determined the upper temperature limits of binary (δPu) phase by dilatometric method. They reported an increase in stability of (δPu) phase at higher temperature by addition of zirconium, reaching a maximum at 55 at.% Zr and 916 K. Further addition of zirconium decreases the temperature of (δPu)/((δPu)+(ε-Pu,β-Zr)) phase boundary to 894 K, the (ε-Pu,β-Zr)↔(δPu)+(αZr) eutectoid temperature. Dilatometric examination of alloys by Ellinger and Land, in the composition range 1 to 5 at.% zirconium indicated a eutectoidal decomposition of (δPu). Based on micrographic and X-ray diffraction analysis, Ellinger and Land placed the eutectoid reaction (δPu)↔ξ+θ at 541 K, at eutectoid composition 3.5 at.% zirconium. They found that at 608 K, (δPu) containing about 22 at.% zirconium transforms congruently into an intermetallic compound, iota (ι).

Marples did not put extra efforts in defining the solubility limit of (δ'Pu) phase. By thermal analysis and dilatometry, he found that (δ'Pu) with even 1.5 at.% zirconium alloys was bi-phasic. He has tentatively put a maximum solubility of ~2 at.% zirconium at the peritectoid, (δ'Pu)↔(δPu)+(ε-Pu,β-Zr). This invariant temperature is given as 758 K in the figure, though he had observed a sharp

arrest at 760 K for the composition 1.5 at.% zirconium. Based on dilatometric results, Ellinger and Land indicated a maximum solubility of zirconium in (δ'Pu) between 1 to 2 at.% zirconium.

2.2.2. Solubility of plutonium in zirconium allotropes

Using the lattice parameter method, Marples [29] reported a maximum solubility of 13 at.% plutonium in α-zirconium at 891 K. He found that solubility of plutonium in zirconium lattice had little affect on the 'a' parameter but increased the 'c' parameter by 0.004 Å per atomic percent of plutonium, therefore, the 'c' parameter was used for determining the phase boundaries. Marples has also determined the phase boundary (αZr)/(αZr)+(δPu) by X-ray diffraction analysis and also found it to be almost vertical. Ellinger and Land [28] determined the plutonium solubility limits in (αZr) at various temperatures by microstructural analysis of homogenised and quenched alloys. By extrapolating this phase boundary, (αZr)/(αZr)+(ε-Pu,β-Zr), to the eutectoid temperature 894 K, they found a solubility of 13 at.% plutonium in (αZr). By X-ray diffraction analysis they found that (αZr) dissolves 13 at.% plutonium even at 873 K. Which indicates that phase boundary (αZr)/(αZr)+(δPu), is almost vertical. They did not determine the solubility at lower temperature. They have also plotted lattice parameters 'a' and 'c' of (αZr) as a function of composition. The plot shows a composition independent parameter 'a', whereas, parameter 'c' increases with increase in plutonium content. Waldron [11] has also reported a solubility up to 13 at.% plutonium in (αZr). According to him, dissolution of plutonium brings down the (βZr)↔(αZr) conversion to 883 K from 1140 K for pure zirconium allotropes. He has also shown the dependence of lattice parameter 'a' and 'c' on the composition for the alloys quenched from 773 K. This comparison shows that the lattice parameter 'a' is independent of the added plutonium in (αZr) but parameter 'c' changes from 5.14 Å for pure zirconium to 5.184 Å for (αZr) with 13 at.% plutonium. Further addition of plutonium does not change the lattice parameter.

Body-centred-cubic allotropes, Pu(ε) and Zr(β) are completely soluble in each other. This binary solid solution phase is labelled as (ε-Pu,β-Zr) in this paper. This phase is very useful in nuclear reactors due to its isosymmetric structure and wide composition and temperature range of stability. Marples [29] reported a miscibility gap, with a maxima at 913 K, in this otherwise continuous solid-solution. He reported a eutectoid at 891 K. Based on his results of thermal analysis and dilatometry, he reported a narrow range for the (ε-Pu,β-Zr)+(δPu) biphasic. Based on dilatometric analysis, Taylor [30] has reported phase boundaries for the (ε-Pu,β-Zr)+(δPu) phase field in the composition range 0 to 10 at.% zirconium. The data was read from a phase diagram given by him. By metallography, cooling curve of thermal analysis and X-ray diffraction methods, Perkins et al. [32] have extensively studied the mode of transition of (ε-Pu,β-Zr) into the (ε-Pu,β-Zr)+(δPu) binary phase field which contains FCC structure of (δPu), in the composition range 5 to 45 at.% zirconium. They have also reported a narrow two phase field of (ε-Pu,β-Zr)+(δPu) which reduces to a congruent point at about 56 at.% zirconium, at 913 K. According to them this suggests a diminished difference between the Gibbs energies of the two phases with increase in zirconium percentage, till it reaches the congruent point, where Gibbs energies of the two phases are equal. They concluded that at low cooling rates the (ε-Pu,β-Zr)↔(δPu) transformation occurs mainly through crystallographically oriented process like Widmanstatten, whereas, at high cooling rate it takes place predominantly by massive transformation.

2.2.3. Intermetallic compounds of Pu-Zr

Coffinberry and Waldron [33] had originally reported a compound Pu_xZr with $x \geq 15$ but later Waldron [11] claimed that all the lines of diffraction pattern of this compound could be explained in terms of another intermetallic compound θ and (δPu). Ellinger and Land [28] have reported an intermetallic compound ξ by X-ray and micrographic analysis in the composition range 2.5 to 3 at.%Zr at 523 K. However, according to crystal structure it should have a composition of 3.4 at.% zirconium corresponding to $Pu_{28}Zr$, as reported by Zachariasen and Ellinger [34]. Using high temperature X-ray diffraction, Ellinger and Land [28] established a peritectoid reaction (γPu)+(δPu)↔ξ, at 545±2 K. This is in agreement with the results of Taylor [30]. Based on the data obtained at the Los Alamos Scientific Laboratory by optical metallography, X-ray diffraction, thermal analysis and dilatometry, Schonfeld [12] has presented some phase diagrams of plutonium alloys,. He has reported a plutonium rich compound that is formed peritectoidally at about 523 K, without fixing its composition. Kutaitsev et al. [35] have determined the phase boundaries of ξ compound by prolonged annealing of metastable (δPu) at temperatures below 573 K. They found this compound to be stable in the composition range ~3 at.% to 5 at.% zirconium and may be described as $Pu_{19}Zr$. They reported that this compound is formed by a peritectoid reaction, (δPu)+θ↔ξ, at ~573 K and decomposes at ~493 K to (αPu) and (βPu). But according them, under normal cooling conditions this compound can be supercooled to room temperature. Taylor [30] prepared Pu-Zr alloys in the composition range 1 to 10 at.% zirconium by melting the weighed amounts of metals on a water cooled hearth in an argon atmosphere. These alloys were further melted in a vacuum induction furnace to form ingots which were heat treated for 24 hrs at 673 K in vacuum and quenched into oil at room temperature to avoid segregation and coring. The alloys were then annealed for 6 weeks at 473 K, and furnace cooled to room temperature. During X-ray analysis and metallographic investigations of these alloys, he observed the compound ξ to be present in all the compositions studied by him from 1 to 8.5 at.% Zr. But alloy with 10 at.% Zr had only θ compound. He explains that the powder pattern of ξ is very complex and is very similar to that of (βPu). Therefore, the diffraction pattern of the compound ξ has many coincident lines with (αPu), (βPu) and θ. Only some of the 2θ values, 35.16, 36.14, 36.56, 37.92, of ξ compound do not overlap with others. This explains reason for missing this compound in some of the earlier investigations. The X-ray pattern of ξ compound given by Taylor is similar to that of Ellinger and Land. In contradiction to Kutaitsev et al. [35], but in agreement with Ellinger and Land, Taylor also found that the compound ξ is stable at room temperature. But according to Taylor, on heating, the compound ξ does not transform peritectoidally to (δPu)+θ as reported Kutaitsev et al. [35] or (γPu)+θ as reported by Ellinger and Land (reported by Taylor, obtained by private communication). Instead it transforms peritectoidally into (γPu)+(δPu). In a later publication, Ellinger and Land [28] also reported that this compound transforms peritectoidally into (γPu)+(δPu). The compound ξ was first reported by Ellinger [36], where he had shown a wide composition range of stability, 5 to 10 at.% Zr. However, in a later publication by Ellinger and Land [28], the nonstoichiometric range of stability of this compound was reduced to 2.5 to 3 at.% Zr. As Ellinger and Land had carried out a thorough and careful phase diagram analysis of the Pu-Zr system for plutonium rich region, therefore, their data was accepted as the most reliable for the present calculations. Most of the later publications have also accepted their work as more reliable, specially in plutonium rich region. In the absence of any reliable data on the non-stoichiometry of the compound ξ, and due to reliable information that its range of non-stoichiometry is very narrow, in present calculations the composition of ξ is fixed as $Pu_{0.973}Zr_{0.027}$.

Bochvar et al. [9] have listed three intermetallics of Pu-Zr, Pu_6Zr (orthorhombic with lattice parameters: a=10.39 Å, b=10.44 Å, c=11.18 Å), $Pu_xZr(x>3)$ (unsolved powder pattern) and $PuZr_2$ (hexagonal with lattice parameters: a=5.060±0.002 Å, c=3.119±0.002 Å). Out of these, first and the last compounds were reported from the work carried out at the Academy of Sciences of the USSR, whereas, the second compound was taken from the work carried out at the Los Alamos Scientific Laboratory. In a publication of Ellinger et al. [37], only two compounds of Pu-Zr are listed. The plutonium rich compound is reported as $Pu_{19}Zr$ instead of Pu_6Zr reported by Bochvar et al. or Pu_4Zr given by Waldron et al. [38]. The zirconium rich compound listed in both publications, Bochvar et al. and Waldron et al., is $PuZr_2$, isostructural with UZr_2.

Taylor [30] also investigated the biphasic region of ξ+θ by dilatometry and X-ray diffraction analysis. By superimposing the room temperature X-ray patterns of ξ and θ on the patterns of alloys ranging from 3 to 10 at.% zirconium, Taylor concluded that the phase field, ξ+θ, extends from 2.9 to 9 at.% zirconium, while Ellinger and Land [28] have shown a very narrow composition range of stability for this biphasic. Based on X-ray diffraction analysis and dilatometry, Taylor has shown a eutectoid reaction (δPu)↔ξ+θ at 543 K and 3.4 at.% zirconium, which is in good agreement with Marples [29] and Ellinger and Land [28]. However, according to Kutaitsev et al. [35] the phase field, (δPu)+ξ, is stable above 546 K in the composition range 2 to 5 at.% zirconium. Whereas, during high temperature X-ray analysis, Taylor did not find these phases in the composition range 2 to 4 at.% zirconium.

Based on X-ray and metallographic analysis, Waldron [11] reported a compound below 603 K with approximate composition Pu_6Zr. Marples [29] has reported a compound of unknown crystal structure with approximate composition Pu_6Zr to be stable over a wide composition range, 12 at.% to 25 at.% zirconium. He has reported an X-ray pattern of the compound with Mo Kα radiation, obtained for the composition 21 at.% zirconium annealed at 593 K and found the lattice to be orthorhombic with cell parameters, a=10.39, b=10.44 and c=11.18 Å. He could not determine the density of this compound because even after long annealing, he could not be certain about the completion of (δPu) to θ conversion. After annealing at 473 K for about 15 weeks a density of 15.86 g/cm^3 was obtained. But according to Marples, true density of θ may be a little higher than this. Based on thermal analysis and dilatometric analysis, he reported a congruent conversion of this compound into (δPu) at 613 K. Whereas, according to Ellinger and Land [28], θ phase is stable only between 6 at.% to 14 at.% zirconium. By high temperature X-ray analysis they determined a peritectoid reaction ι+(δPu)↔θ, at 587 K They found that compositions of (δPu) and θ in this peritectoid reaction are very similar. They could not determine the crystal structure of θ compound but from X-ray data they suggested that this compound should have a structure similar to θ compound of Pu-Hf system. The θ compound of Pu-Hf is orthorhombic with lattice parameters: a = 10.415±0.005 Å, b = 10.428 Å, c = 11.245 Å, which is in good agreement with X-ray analysis results of Marples.

Instead of showing a wide composition range for the compound θ as suggested by Marples [29], Kutaitsev et al. [35] and Bochvar et al. [9], for the first time Ellinger and Land [28] reported a narrower range of stability of the compound θ and formation of another compound iota (ι) in the composition range 19 to 24 at.% Zr. According to them, ι transforms congruently into (δPu) at 608 K and 22 at.% zirconium and is readily distinguishable from the compound θ. Though they did not determine the crystal structure of this compound, they have listed a low angle X-ray powder data for this compound. Marples [29] and Bochvar et al.[9] did not mention the existence of this compound.

They have reported the compound θ in the above mentioned composition range. But they had also missed the presence of the intermetallic compound ξ, which was later confirmed in many other publications [35,39], therefore, relying on the work of Ellinger and Land [28], the intermetallic compound ι was also considered in present calculations. General features of the phase diagram are similar to a previous publication of Ellinger and Land [28]. Except for the inclusion of the plutonium rich compounds ξ and ι in present calculations, rest of the features of present phase diagram are similar to that given by Marples [29].

Marples has reported a stoichiometric, zirconium rich compound, kappa (κ) at about 75 at.% zirconium. The X-ray pattern of an alloy containing 75 at.% zirconium, annealed at 473 K for three weeks, is listed by Marples. The pattern was indexed on the basis of an hexagonal cell with lattice parameters, a =5.055 Å and c = 3.123 Å and space group P6/mmm and the structure is disordered C_{32} AlB_2 type, similar to that of UZr_2. He found that on heating this compound to 653 K, it decomposes peritectoidally to (αZr) and (δPu). But thermal analysis method could not be used for determining this peritectoid temperature. Bochvar et al. [9] have reported this as $PuZr_2$ compound with hexagonal structure similar to UZr_2 and lattice parameters, a = 5.060±0.002 Å, c = 3.119±0.002 Å. In a publications by Schonfeld [12], based on Russian work, a phase diagram of Pu-Zr is given in which compound κ is shown with a narrow non-stoichiometry. According to this phase diagram, the compound κ is formed by a eutectoid reaction, (δPu)↔κ+(αZr), at 688 K and on heating it gets converted congruently in (δPu). Both Bochvar et al. and Schonfeld [12] have shown a narrow non-stoichiometry in κ compound. Waldron [11] has reported some of the plutonium work carried out at Harwell. According to this publication, a zirconium rich compound $PuZr_2$ is found at temperatures below 653 K. The diffraction pattern of this phase can be indexed on the structure proposed by Silcock [40] for UZr_2, as hexagonal with space group $P\bar{6}m2$ with 3 atoms per unit cell having a=5.055±0.005 Å and c=3.123±0.005 Å. Marples obtained this compound after annealing an alloy containing 75 at.% zirconium at 473 K for three weeks. They have reported that this alloy attained equilibrium at very slow rates at such low temperature. Suzuki et al. [31] could not get this compound even after heat treatment of the alloy at 625 K for 8 days. Ellinger and Land [28] have observed that they could get this compound only in the presence of impurities like oxygen. They observed that this compound was not found in massive alloys but was sometimes observed on the surface of the filings heated in evacuated silica capillary tubes. They found that when a bulk sample of 75 at.% zirconium was treated at 1123 K for a week, then its filings treated at 1123 K for a minute gave strong patterns of κ phase. But the filings of the same sample treated at 673 K for 5 minutes to stress relieve showed only (δPu) and (αZr) phases. Lauthier et al. [41] have also reported that this compound can be formed only in presence of oxygen which improves the kinetics by accelerating the diffusion process. This agrees with Marples observation. In most of the reported literature on Pu-Zr system, Waldron [11], Schonfeld [12], Waldron et al. [38] and Bochvar et al. [9] etc., the compound κ is considered to be a stable compound. O'Boyle and Dwight [42] have studied U-Pu-Zr ternary system by electron microprobe, X-ray diffraction and optical micrography. They observed that UZr_2 and $PuZr_2$ form a complete series of solution or plutonium shows extensive solubility in UZr_2 compound. This can be understood only if Pu-Zr binary also has a stable kappa phase, isostructural to UZr_2. According to the zirconium rich partial phase diagram given by Marples, κ+(δPu) phase boundary were determined by X-ray diffraction method at approximately 60, 65 and 70 at.% zirconium. In this diagram, Marples has shown that the first two compositions show the presence of (δPu) and κ phases at three to four temperatures. But alloy with 70 at.% zirconium is shown to contain these phases only at one temperature. Marples

[29] has shown by X-ray diffraction analysis that the alloy with approximately 75 at.% zirconium is pure κ at ~550 K, but same composition alloy investigated by him at ~ 430 K is reported to have three phases in equilibrium. This may indicate some doubts on the actual composition of κ and the phases in equilibrium with it. Therefore, based on the reports of stability of (U,Pu)Zr_2 alloy and isostructure of $PuZr_2$ and UZr_2 compounds, in present calculations, it was assumed that $PuZr_2$ is a stable compound with slight non-stoichiometry in the composition range 66 to 70 at.% zirconium, but it does not convert congruently into (δPu), instead undergo peritectoid decomposition into (δPu) and (αZr).

Marples [29] determined the phase boundaries of (δPu)/κ and (αZr)/κ by X-ray diffraction. But according to him, boundaries between (αZr)/κ were not reliable as the equilibrium was not attained in the allotted time for annealing. In case of (δPu)/κ phase field, sharp X-ray patterns were obtained for κ but very blurred pattern were seen for (δPu). After annealing the alloy with 60 at.% zirconium at 473 K and heating it at 601 K for several days, the X-ray pattern showed mainly (δPu) and very little κ. From this he analysed that the alloy was very close to (δPu)/(δPu)+κ boundary. Marples determined the eutectoid temperature of (δPu)↔θ+κ, by annealing alloys at 463 K for ~3 weeks and then heating them to successively higher temperatures to establish the temperature where the quenched samples indicated that the eutectoid temperature was passed. They found this between the temperatures 533 K to 548 K. The eutectoid composition of 55 at.% zirconium given by them was not determined accurately. It was obtained by the intersection of (δPu)/(δPu)+θ and (δPu)/(δPu)+κ boundaries with eutectoid temperature. In dilatometric experiments, a sample containing 45 at.% zirconium, annealed at 473 K for three weeks, gave a slight kink at 533 K in the expansion curve. The phase boundaries of (δPu)+θ phase field were determined by Marples by X-ray diffraction method. However, he attaches some unreliability to his data due to sluggishness of the equilibrium reaction. In contrast thermal analysis and dilatometry gave rather sharp arrest during heating, which could be due to superheating of θ compound before decomposing to (δPu).

2.2.4. Liquidus-solidus equilibrium

Marples [29] has investigated liquidus-solidus curves of this system using thermal scanning. The solidus was studied up to ~ 60 at.% zirconium, whereas, only three data points were reported for liquidus curve. The reported solidus data shows considerable scatter while the two liquidus data points obtained during cooling are completely inconsistent with the phase diagram given in his publication. Two liquidus points with a composition difference of almost 10 at% Zr, are shown at same transition temperature, thus clearly indicating the inconsistency of the liquidus data. The liquidus points were obtained by Marples during cooling cycle at the rate of 5 ^{o}C/minute, where the specimen was contained in alumina crucible and thermocouple was also sheathed with an alumina tube. The discrepancy in liquidus data could be due to reaction of the liquid alloy with alumina container, as reported by the author. Bochvar et al. [9] have drawn liquidus-solidus curves in a figure of Pu-Zr phase-diagram. But experimental method or the source of experimental data points used for drawing these curves are not discussed in their publication. The curves drawn by Bochvar et al. indicate a steep rise in solidus curve as zirconium content increases, whereas, solidus drawn by Marples indicates a flatter temperature increase with increase in zirconium content. The difference in the solidus curves of Bochvar and Marples increases with increase in zirconium content. Out of the two liquidus data points given by Marples, one is quite in agreement with the Bochvar et al., whereas, the other one is completely off. As a result of the difference in the slopes of the solidus curves of these two

publications, the liquid-solid biphasic region is broader in Marples phase diagram compared to Bochvar et al. The solidus points given by Taylor [30] for an alloy composition ≤ 10 at % Zr, are in reasonable agreement with Bochvar et al. [9] but do not differ much from solidus shown by Marples. However, liquidus points given by Taylor indicate a much steeper increase with increase in zirconium content, compared to either Bochvar et al. or Marples. Another set of liquidus and solidus temperatures for Pu-Zr system was picked up from a liquidus-solidus phase diagram of Pu-U-Zr given in an MLM report [43]. The solidus points are in reasonable agreement with that of Bochvar et al. [9], however, liquidus is higher than all other reported works discussed here [9,29,41]. In agreement with previous optimizations by Leibowitz et al. [26] and Shunk [44], extensive analytical investigation of Pu-Zr solidus-liquidus by Marples was given more weightage during present calculations.

2.2.5. Thermodynamics of Pu-Zr system

Sandenaw and Harbur [39] have determined heat capacity of ξ compound, containing 2.55 at.% Zr, in the temperature range 15 K to 373 K. However, in present calculations, the compound ξ was assumed to contain 2.7 at.% Zr. Therefore, the heat capacity data given by Sandenaw and Harbur in the temperature range 300 K to 373 K was used but for the composition 2.7 at.% Zr.

Maeda et al. [45] have measured partial vapour pressures of plutonium over Pu-Zr alloys of the compositions, 20, 50, 60, 75, 82 and 94 at.% Zr, in the temperature range 1400-1900 K, using a quadrupole mass spectrometer with a knudsen effusion cell. In their plots of activity of plutonium vs. composition they found activity coefficient near unity, thus concluding that the Pu-Zr alloys might show near ideal behaviour, in contrast to U-Zr alloys.

2.2.6. Discussion

Based on the above mentioned phase diagram and thermodynamic data, excess Gibbs energies of the binary Pu-Zr phases were calculated as a function of temperature and composition. The coefficients of Redlich-Kister polynomial as given in equations (3) and (4) are listed in the table 8. The temperatures and compositions of the binary phases at invariant equilibria, calculated using these optimized Gibbs energy values, are compared with literature values in the table 9. The calculated phase diagram of Pu-Zr binary is given in figure 4. A low temperature phase diagram, 500 to 1150 K, is given in figure 5 to compare the calculated and experimental phase boundaries of (ε-Pu,β-Zr)/(δPu), (δPu)/(αZr), (δPu)/ι, (δPu)/κ and ι/κ. A plutonium rich partial phase diagram is given in figure 6 to compare experimental and calculated phase boundaries of plutonium rich solid phases.

According to present calculations, the compound θ is formed by a peritectoid reaction, ι+(δPu)↔θ, at 584.2 K with (δPu) and θ compositions, 12.85 at.% Zr and 14.9 at.% Zr, respectively. Ellinger and Land [28] have reported this peritectoid at ~ 587 K, with almost the same equilibrium compositions of θ and (δPu). Whereas, Marples has reported a congruent transition of (δPu) in θ compound at 618 K in the phase diagram and 613 K in the text. The boundary compositions of the compound θ are represented by dashed line in Marples phase diagram, indicating uncertainty in this region.

Ellinger and Land [28] have reported a congruent transition of (δPu) into ι compound at ~608 K and ~22 at.% Zr. Based on the optimized Gibbs energy values of present calculations, this congruent transition was found at 608 K and 22 at.% Zr. As mentioned earlier, the wide composition range of stability of the compound θ reported by Marples [29] and Bochvar et al. [9] included the compounds ι and θ reported by Ellinger and Land [28]. Therefore, it can be assumed that the congruent transition of (δPu) into the compound θ, reported by Marples at 613 K and ~20 at.% Zr, is in fact (δPu) ↔ ι congruent transition reported by Ellinger and Land [28]. According to Bochvar et al., this transition occurred at temperature below 623 K and in the composition range 12.1 to 20.6 at.% zirconium. All these data are in reasonable agreement with each other if we consider that the compound θ and ι could not be distinguished by the previous authors.

In figure 7, calculated and experimental liquidus-solidus of Pu-Zr system are compared. As seen in the figure, liquidus as well solidus data points given by Taylor [30] are in reasonable agreement with calculated solidus-liquidus. Except for solidus data of Bochvar et al. [9], which deviates from calculated solidus curve for the composition >30 at.% zirconium, all other solidus data reported in literature are in reasonable agreement with solidus calculated from present set of Gibbs energy polynomials of Pu-Zr system. Marples' data is scattered but it is in general agreement with calculated solidus. On the other hand, liquidus curve given by Bochvar et al. is at lower temperatures compared to the calculated one, whereas, liquidus temperatures given in the MLM report are too high. Only two liquidus data point out of three data points given by Marples are close to the calculated liquidus. Liquidus data of Taylor is also in good agreement with the calculated one. There is a reasonably good agreement in the calculated liquidus and solidus of Leibowitz et al. [26] and the present values. Due to higher solidus temperatures and lower liquidus temperatures given by Bochvar et al. [9] compared to present calculation, the biphasic region of solid-solution+liquid-solution is very narrow in the phase diagram given by Bochvar. On the other hand, the calculated liquidus and solidus temperatures given by Leibowitz et al. [26] are slightly lower than the present calculated values but the temperature range of stability of the biphasic region, for a given composition of the alloy, remains almost same in both. As in present calculations, Maeda et al. [45] and Leibowitz et al. [26] have also considered ideal liquid solution and regular solid-solution behaviour. Present value of excess Gibbs energy of G^E(solid-sol) = (5204.89 + 0.67574 T) $X_{Pu}X_{Zr}$ (J/mol) is in-between that of $4500X_{Pu}X_{Zr}$ (J/mol) given by Maeda et al. and $6700X_{Pu}X_{Zr}$ (J/mol) given by Leibowitz et al. In figure 8, plutonium activity of the liquid and solid-solution alloys measured by Maeda are compared with present calculations. The horizontal line in the figure indicates the bi-phasic liquid+solid-solution region, where, plutonium activity is constant. It can be seen from the figure that with increase in temperature, activity coefficient of plutonium reported by Maeda et al. comes closer to unity. In present calculations, excess Gibbs energy of the BCC solid-solution phase shows a very small temperature dependence, whereas, activity data reported by Maeda et al. [45] shows considerable temperature dependence. The excess Gibbs energy of the liquid Pu-Zr was assumed to be zero in present calculations. Though experimental data of plutonium activity in liquid Pu-Zr solution by Maeda et al. [45] showed slight temperature dependence, they also assumed ideal liquid solution behaviour during modelling. Present calculations and experimental data reported by Maeda et al. indicate that the activity coefficients of plutonium in BCC solid-solution at 1823 K and 1673 K are more than unity thus indicating a positive deviation from ideality.

The heat capacity values of ξ intermetallic compound, with 2.7 at.% Zr, calculated from optimized Gibbs energy, in the temperature range 300 K to 400 K are compared with that of Sandenaw

and Harbour [39]. Heat capacity values of the compound calculated by Newmann-Kopp's additivity rule for 2.7 at.% Zr alloy are also shown in the figure 9. It can be seen that heat capacity values calculated from optimized Gibbs energy values are reasonably close to Newmann-Kopp's heat capacity values as the calculated excess heat capacity of ξ is only ~5.8 J/mol.K. However, as seen in figure 9, experimental values are lower than even Newmann-Kopp's values.

2.3. Uranium-zirconium

To calculate the optimized Gibbs energies of this binary system, Gibbs energies of all the allotropes of uranium and zirconium were required. Allotropes of uranium and zirconium are already discussed in section 2.1 and 2.2, respectively. The Gibbs energies of alpha allotropes of uranium and zirconium are given in equations 7 and 8, respectively. The Gibbs energies of transitions from alpha to higher temperature allotropes of uranium and zirconium are listed in tables 2 and 6, respectively. The Gibbs energies of hypothetical U(κ) and Zr(κ) allotropes of uranium and zirconium, which combine to form 'κ-UZr_2', intermetallic compound in U-Zr binary system, were estimated from the Gibbs energies of alpha allotropes of the respective elements. A temperature independent function of Gibbs energy for the hypothetical Uranium(κ) phase was calculated by Ogawa and Iwai [27] by extrapolating the Gibbs energy of U(α) to the transition temperature of U(κ) assuming U(κ) undergo transition to U(γ) at 933 K. Similarly, a temperature independent Gibbs energy of transition from Zr(α) to Zr(κ) was estimated by Sanshez and de Fontaine [46], assuming that Zr(κ) undergoes transition to Zr(β) at 890 K. These hypothetical transition values of U(κ) and Zr(κ) from their respective alpha allotropes are listed in table 2 and 6, respectively.

Uranium-zirconium binary system is the best studied system among the three binaries under investigation in present calculations. The reason for most of these investigations was the use of uranium as reactor fuel. By adding small amounts of alloy elements like, molybdenum or zirconium, structural stability of uranium can be significantly increased. Additions of small amounts of zirconium in uranium modify the kinetics of beta or gamma phase to produce randomly oriented grains with fine grain size. This reduces the elongation tendency of orthorhombic, alpha-uranium during thermal cycles. It was observed by Zegler and Chiswik [47] that a minimum of 5 at.% zirconium was required to be added in uranium to attain fine-grained acicular structure, which on water quenching from gamma phase, resulted in negligible length changes and the rod surface remained smooth even after thousand cycles. The alloy with 13 at.% zirconium showed negligible deformation and no surface roughening even on furnace cooling. It was found that the addition of even higher amounts of these alloys elements (Mo/Zr) stabilize the cubic gamma phase to a larger extent thus circumventing the intrinsic instability of orthorhombic alpha phase of uranium. These gamma alloys with higher zirconium content were studied extensively for fast reactors, where increase in the melting point is another added criteria.

As discussed in later parts of the section, reasonably reliable phase diagram data is available in literature. The phase diagram of uranium-zirconium has been studied quite extensively by a number of investigators [48-50]. The system was recently assessed by Sheldon and Peterson [51], Ogawa and Iwai [27] and Leibowitz et al [52]. The main features of this phase diagram are: (i) presence of a large homogeneous solid solution (γ-U,β-Zr) (also given as ε in later part of the text) over the complete composition range, formed by mixing of U(γ) and Zr(β) (ii) a small miscibility gap in (ε-Pu,β-Zr)

solid-solution on uranium rich side (iii) a non-stoichiometric intermetallic compound, κ-UZr_2, on zirconium rich side (iv) a very small solubility of uranium (α/β) and zirconium (β) metals in each other.

2.3.1. Solubility of Zr in (αU) and (βU)

Unlike gamma-uranium and beta-zirconium which form a solid-solution over the complete composition range, alpha and beta phases of uranium dissolve very small amounts of zirconium and alpha phase of zirconium also dissolves small amount of uranium. Summers-Smith [49] determined solubility of zirconium in beta-uranium metallographically. He found that at the monotectoid temperature, ε↔ε'+(βU), beta-uranium contains 2.5±0.5 at.% zirconium. But he could not determine solubility limit at eutectoid temperature by metallography. Using dilatometry, he found that tentative eutectic composition of beta-uranium is 1.5 at.% zirconium. Summer-Smith has suggested that maximum solubility of zirconium in alpha-uranium is less than 1 at.%. However, owing to the fine nature of the microstructures, he was not able to determine this solubility limit with certainty. Zegler [50] determined the solubility limits of zirconium in alpha and beta uranium and that of uranium in alpha-zirconium by disappearing phase technique. He reported a solubility of zirconium in alpha-uranium slightly more than 0.55 at.% at beta eutectoid temperature, 935 K. It decreases with temperature to 0.23 at.% at 773K. In beta uranium, maximum solubility is slightly less than 1.06 at.% at monotectoid reaction temperature, 966 K and decreases to 0.78 at.% zirconium at beta eutectoid temperature. Chiswick et al. [53] have reported metallurgical behaviour of uranium alloys with 5 and 7.5 at.% zirconium. They observed the presence of (βU)+ε'' phase field with fine spheroidal structure and lowest hardness. According to them, tempering in, and water quenching from this region gives the most stable alloys compared to the ones tempered in and quenched from (βU)+ε' phase field, above 966 K. Though they have not indicated clearly the transition temperatures and solubility limits of zirconium in uranium, but their experiment indicates that the (βU) to (αU) transition is a eutectoid reaction and not a peritectoid reaction, as reported by Rough and Bauer [54]. A phase field with (βU)+ε'' will be stable only in case of a eutectoid transformation. The phase fields, (βU)+ε' and (αU)+ε'', will be stable in case of peritectoid reaction. Chiswik et al. [53] found (βU)+ε' phase field above 966 K, formed by monotectoid reaction ε'↔ε''+(βU). The acicular microstructure obtained by tempering in and quenching of (βU)+ε', was found to be unstable and hard compared to the one obtained from (βU)+ε''. Based on dilatometry and high temperature X-ray diffraction results, Rough and Bauer [54] have also reported that (βU)+ε'' phase field is stable between the monotectoid temperature and 935 K. They also reported the absence of (αU)+ε phase-field.

2.3.2. Solubility of uranium in (αZr)

Solubility limit of 0.3 at.% uranium in alpha-zirconium at the eutectoid temperature was determined by McGeary [55] using differential dilatometry of a series of alloys. Based on metallography and autoradiography data Summers-Smith [49] determined the solubility limit of uranium in (αZr). He found that maximum solubility of uranium in alpha-zirconium is 1.0±0.5 at.% at the eutectoid temperature, 879 K. Chiswik et al. [53] have reported solubilities of 0.52 at.% Zr at 935 K in (αU) and 1.06 at.% Zr in (βU) at 966 K. By studying changes in the volume percentage of phases as a function of oxygen and nitrogen impurity contents, Rough and Bauer [54] could extrapolate phase boundaries of U-Zr binary to zero oxygen and nitrogen impurities. He observed that U-Zr alloy with 83

at.% Zr is a single phase solid solution, (γ-U,β-Zr), but on addition of oxygen or nitrogen impurities, (αZr) precipitates out and it becomes biphasic with (αZr)+ε. Therefore, dissolution of oxygen and nitrogen in (αZr) broadens (αZr)+ε phase field. However, he observed that due to limited dissolution of nitrogen in zirconium, its effect is less than that of oxygen. Rough et al. [56] also showed that dissolution of oxygen and nitrogen stabilises (αU) and (αZr) phases at the expense of ε solid-solution and κ-intermetallic compound. According to Bauer et al. [57], at 933 K, the phase boundary of (αZr)+ε phase field is at 85 at.% zirconium. Bauer et al. [57] has reported a solubility of less than 0.3 at.% uranium in (αZr).

2.3.3. ε+ε' miscibility gap and solid state transformations

Presence of two solid-solution phases in the region of miscibility gap was first time reported by Rough and Bauer [54] and Summer-Smith [49] by metallographic, dilatometric and high temperature X-ray analysis. Summer-Smith analysed samples at the interval of 5 at.% zirconium and confirmed by X-ray analysis that the solid-solution obtained at 1273 K, in the composition range 40 at.% to 90 at.% Zr, had body-centred cubic structure and the parameters of the phase varied linearly with composition. At 973 K they found this single phase alloy for the compositions, 15 at.%, 20 at.% zirconium and composition range, 55 at.% to 75 at.% Zr. Using metallographic and dilatometric analysis, Summer-Smith placed monotectoid transformation of (γ-U,β-Zr) at 966±3 K and 14.5±0.5 at.% zirconium. Later this region of phase diagram was extensively studied by Zegler. Based on microstructural analysis, he determined the compositions of the two (γ-U,β-Zr) phases in equilibrium at 973 K to be 17.5 at.% and 50.0 at.% zirconium, and 21.5 at.% and 38.0 at.% zirconium at 983 K. Based on his metallography data he suggested that the peak of the miscibility gap is between 983 K and 998 K. Based on the data of compositional limits at 973 K and 983 K, he gave a peak at 995 K and 29.8 at.% zirconium. Similarly by extrapolating the phase boundary of (ε+β)/ε phase boundary and ε'+ε'' phase boundary to lower temperature, he placed monotectoid composition at 10.95 at.% Zr. Chiswik et al. [53] have maintained the equilibrium temperature of the monotectoid at 966 K as given by Zegler, but relocated the (ε'+ε'') phase boundaries to 13.2 at.% and 42.3 at.% Zr at monotectoid. They also noted that the presence of impurities of oxygen and nitrogen enlarges the composition limits of miscibility gap and affect monotectoid temperature. The (γ-U,β-Zr) phase is the most relevant phase for the nuclear fuel. It has body-centred cubic structure.

Based on dilatometric results, Summer-Smith [49] concluded that the second transformation of (γ-U,β-Zr) solid-solution on cooling was due to uranium alpha-beta eutectoid reaction at 935±2 K. The third transformation was also a eutectoid reaction. He placed it at 879±3 K and 69.5±0.5 at.% zirconium. Whereas, Zegler [50] carried out thermal analysis of 2.57 at.% zirconium alloy at a heating rate of 1 K/min. He placed uranium alpha-beta eutectoid reaction at 938 K. Both Summer-Smith and Zegler found that the arrests observed during cooling cycles were not reliable. On the contrary Rough et al. [56] and Philibert et al. [58] suggested a peritectoid transformation to alpha-uranium from beta-uranium at 973 K, therefore, indicating a very narrow range of stability of beta-uranium in the binary phase diagram. But later works by high temperature X-ray analysis of Howlett and Knapton [59], Craik et al. [60], Lagerberg [61], Virot [62], and heat capacity measurements by Fedorov and Smirnov [63], have strongly favoured the results of Summer-Smith and Zegler showing a monotectoid transformation, ε↔ε'+U(β) and a eutectoid transformation at lower temperature, (βU)↔(αU)+ε. Lagerberg [61] has shown by DTA analysis of uranium rich alloys that the alpha-beta transition

temperature of uranium increases with addition of zirconium. Therefore, he suggested that the eutectoid reaction (βU)↔(αU)+ε, as suggested by Howlett and Knapton [59], should be replaced by a peritectoid reaction (βU)+ε↔(αU), at slightly higher temperature. However, they suspected that this increase in (αU) to (βU) transition temperature may be attributed to delayed nucleation of (βU) due to the presence of zirconium.

2.3.4. Intermetallic compound, κ-UZr_2

The system has only one intermetallic compound, κ, on zirconium rich side of the system. Summer-Smith [49] did not observe this compound in his extensive investigation of uranium-zirconium system. However, Mueller [64] suspected that this binary system has a metastable intermediate compound. Later, Rough et al. [56] and Duffey and Bruch [65] established it as a stable intermetallic compound. With the help of high temperature X-ray diffraction and thermal analysis, Rough et al. [56] were able to demonstrate that κ↔ε phase transformation is a reversible process. They also found that κ-compound is not just a transition phase in the decomposition of ε solid-solution into (αU)+(αZr), but it is a stable compound. According to them, destabilisation of the compound 'κ' by oxygen contamination resulted in the confusion in establishing the presence of this compound in U-Zr binary system. Bauer et al. [57] carried out X-ray diffraction analysis of the compound obtained by transformation of single crystal of ε-solid-solution. The high temperature, single crystal of (γ-U,β-Zr) was body-centred cubic, which on cooling transformed to twinned crystals where c-axis of the hexagonal cell was oriented along the eight possible (111) directions of the parent cubic cell, resulting in apparent cubic symmetry. They have assigned it a primitive hexagonal structure with 'a' and 'c' parameters as 5.03 Å and 3.08 Å, respectively. According to Bauer, the structure of UZr_2 is partially ordered with zirconium atoms at 0,0,0 position and zirconium and uranium atoms located randomly at 1/3, 2/3, 1/2, and 2/3, 1/3, 1/2 positions. This randomisation in the position of uranium and zirconium atoms causes reasonable non-stoichiometry in the compound. Bauer assigned it a space group of P6/mmm, where the structure is partially disordered C 32-type AlB_2 structure. He detected a change in thermal expansion and electrical resistivity values of this compound below 673 K. However, he suggested that this change was not due to change in the crystal symmetry. According to him, it may be due to change in positioning of atoms in the lattice or change in degree of order. Holden and Seymour [66] prepared samples of the composition 64, 73, 80 and 90 at.% Zr and carried out X-ray diffraction, metallography and electrical resistance studies on them. They observed that samples with 64, 80 and 90 at.% Zr had varying amounts of second phase along with κ-intermetallic compound but sample with 73 at.% Zr was single phase at all temperatures up to 1173 K. However, they observed that when the sample was quenched from above 898 K, it was isotropic, whereas, when quenched from temperatures at or below 868 K, it was optically active. From electrical resistance measurements also they placed the transition temperature at ~855 K. They have given the lines observed from X-ray diffraction. They have indexed this pattern as BCC with a=10.68 Å. However, later Silcock [40] interpreted their lines differently and suggested that the κ-intermetallic compound is in fact a twinned crystal with four hexagonal cells giving and appearance of a large BCC structure. He gave the lattice dimensions as a=5.03 Å and c=3.08 Å. Holden and Seymour [66] further analysed that all simple body-centred-cubic solid-solutions containing large quantities of titanium or zirconium tend to form similar type hexagonal cell, however, it is rarely stable. The Structure of delta phase has also been studied and confirmed as primitive hexagonal by Boyko [67] and Mueller et al. [68]. Boyko [67] examined the crystal cut from arc-melted ingot of alloy with equal weights of uranium and zirconium. According to

him, transformation of single crystal of the body-centred cubic ε phase, which is an unordered solid-solution, yields twinned crystal with four hexagonal cells oriented as $[0001]_\delta \,|\, [111]_\gamma$, $[11\bar{2}0]_\delta \,|\, [1\bar{1}0]_\gamma$. According to him, these hexagonal cells oriented in this manner cause an appearance of cubic structure in X-ray photographs, a phenomenon observed in ω phase of Ti-Cr and Ti-16at.%V alloys. He has given lattice parameters as, c=3.08 Å and a=5.03 Å. Barnard [69] measured electrical resistivity and magnetic susceptibility of this compound. His data also supports hexagonal structure of the compound. Makarov [70] has proposed that κ-compound is isotypic with hexagonal Ni_2In.

Bauer [71] reported an extensive study of transformations from solid-solution phase to intermetallic compound, in the composition range of 46 to 100 at.% zirconium, using X-ray diffraction, dilatometric, dynamic-modulus, hardness, resistivity and metallography techniques. He found that ε with 72 at.% zirconium transforms into pure intermetallic compound, whereas other alloys in the composition range 46 to 91 at.% Zr get isothermally transformed into the intermetallic compound along with precipitates of either alpha uranium or alpha zirconium, depending upon the composition. Whereas, alloys containing more than 91 at.% zirconium, transform into (αZr) on quenching. Based on these studies, Bauer concluded that transformation from epsilon to intermetallic compound by quenching above martensite temperature is diffusion controlled growth of compound nuclei. Whereas, below martensite temperature, it is controlled by strain activated growth of zirconium nuclei for zirconium rich alloys. But in case of alloys with 96.4 and 95.4 at.% zirconium, a transformation of solid-solution just above martensite temperature resulted in bainitic type alpha zirconium, indicating a diffusion controlled growth of (αZr) nuclei. Bauer [71] observed that the presence of oxygen or nitrogen impurities severely constricts the composition limits of solid-solution phase and intermetallic compound.

Holden and Seymour [66] confirmed the presence of this compound by metallographic, electrical resistance and X-ray analysis. They concluded that the κ compound is formed on cooling from body-centred cubic epsilon phase by ordered-disordered transformation between 868 and 883 K. Though they indicated a non-stoichiometry of approximately 63-79 at.% Zr, they could not define it reliably. The wide non-stoichiometry of this compound was later determined by Duffey and Bruch [65] using alloys of 15 different compositions in the range 57-86 at.% Zr. They carried out thermal analysis, metallography and hardness studies on these alloys to determine the transformation temperature and composition range of stability of the compound. They placed the transformation temperature on uranium rich side at a peritectoid temperature, 890 K and peritectoid composition of the solid-solution as 62.5 at.% Zr. On zirconium rich side it transforms at a eutectoid, 879 K for gamma composition as 76 at.% Zr. According to them, the maximum solubility of zirconium in κ-compound is 73 at.% Zr, which is almost independent of temperature. On the other hand, they reported a maximum solubility of 37.5 at.% uranium in κ-compound at the peritectoid temperature, 890 K, which decreases to 34 at.% uranium at 833 K. As their samples had 0.3 at.% oxygen, they expected very small constriction effect of oxygen on the κ-compound phase boundaries. Howlett and Knapton [59] investigated the nonstoichiometry of κ-compound by metallography and M. Akabori et al. [72] by electron probe micro-analysis. Though non-stoichiometric composition limit on uranium rich side of κ compound determined by these authors agree with each other, there is a discrepancy in the values for zirconium rich limit. The non-stoichiometric range of ~63-73 at.% Zr as determined by Duffey and Bruch [65] is much narrower than ~63-79 at.% Zr given by Howlett and Knapton [59] or ~64-80 at.% Zr given by

Akabori et al. [72]. Ivanov and Bagrov [73], Bauer [71], and Wisnyi and Pijanowski [74] have reported a nonstoichiometry range of 65-79 at.% Zr, 70-76 at.% Zr and ~65-72.5 at.% Zr, respectively.

2.3.5. Liquidus-solidus equilibrium

The solidus and liquidus equilibrium was investigated by Summers-Smith [49] using optical pyrometer and microstructural analysis. Liquidus temperatures were determined for the composition range 40 to 100 at.% zirconium, whereas, solidus temperatures were measured for the compositions 10, 30 and 50 at.% zirconium. The liquidus-solidus curves given by Massalski [75] were based on the data given by Summers-Smith [49]. Leibowitz et al. [26] have reported solidus and liquidus temperatures for a single alloy of composition 19.3 at.% zirconium. Their values are in reasonable agreement with the Summer-Smith data. Kanno et al. [76] and Ohmichi [77] have also reported liquidus-solidus equilibrium temperatures for some compositions, calculated from uranium activity measurements.

2.3.6. Thermodynamics

Fedorov and Smirnov [78] measured uranium activity of U-Zr alloys in the temperature range 1033-1183 K from EMF of fused salt cells. The average temperature of their measurement is 1073 K. At this temperature (γ-U,β-Zr) solid-solution is the stable phase. Fedorov and Smirnov calculated integral Gibbs energy of mixing of U-Zr at 1073 K from the partial Gibbs energy values. Kanno et al. [76] measured uranium partial pressures over (liquid-U,Zr) and (γ-U,β-Zr) solid-solution in the temperature range 1700-2060 K by high temperature mass spectrometric technique. From their experimental data they inferred that uranium activity shows a negative deviation from ideality in liquid as well as solid-solution alloys. The deviation from ideal behaviour was particularly high in uranium rich liquid alloys. Maeda et al. [79], have reported activity of uranium in U-Zr alloys containing 24.4 and 39.3 at.% Zr, in the temperature range 1673-1873 K, using Knudsen cell-mass spectrometer. Based on the break in the vapour pressure vs. 1/T curve, they indicated a liquidus transition at 1693 K and 1793 K, respectively for the above compositions.

Heat capacities of the solid U-Zr alloys in the temperature range 293-1273 K, measured by pulse method, were reported by Fedorov and Smirnov [63]. The heat capacity values for pure uranium, zirconium and U-Zr alloys with 13, 41, 61, 73 and 89 at.% zirconium were presented in the form of polynomial equation of the type $C_P = A+BT+CT^{-2}$ and were also plotted as C_p vs. temperature. Most of their heat capacity measurements were in biphasic region. From the breaks in the heat capacity plots they determined the transition temperatures. The heat capacity of 89 at.% zirconium alloy showed a break at 878 K, corresponding to the transition (γ-U,β-Zr)↔ (αZr)+κ-UZr_2. The alloy with 73, 61, 41 and 13 at.% zirconium showed a break at 883 K corresponding to the transition (γ-U,β-Zr)+(αU)↔κ-UZr_2. The alloys with 41 and 13 at.% zirconium also showed transitions at 935 K and 968 K which could be due to the transitions (βU)↔(αU)+(γ-U,β-Zr) and (γ-U,β-Zr)↔(γ-U,β-Zr)'+(βU), respectively. The heat capacities values of these measurements could not be used because most of these measurements were done in biphasic regions. However, one of the compositions studied by them was a uranium-zirconium alloy with 73 at.% zirconium, composition of the intermediate compound, κ. The temperature dependence of the heat capacity of this compound was given as:

$$C_p\ (J/mol.K) = 12.9+3.5\times10^{-2}T+4.1\times10^{5}T^{-2} \quad (9)$$

Takahashi et al. [80] have also reported heat capacities of various U-Zr alloys using laser flash technique. They have carried out measurements for 14, 35, 72 and 91 at.% zirconium. For the reason mentioned above, only heat capacity values for 72 at.% zirconium, corresponding to κ-UZr_2, were used in present calculations.

Heat capacity of the BCC solid-solution, given by Fedorov and Smirnov [63], is independent of temperature and shows a very small composition dependence. The value was read from a small plot, and is approximately 40 J/mol.K. Nagrajan et al. [81] determined enthalpy of formation of the intermetallic compound κ-(U,Zr) by high temperature solution calorimetry using liquid aluminium as the solvent. They reported enthalpy of formation, -4.0±10.1 kJ/mol at 298 K.

2.3.7. Discussion

All the important phase equilibrium data and thermodynamic data of U-Zr system available in literature along with reported optimization calculations are listed in table 10. The optimized excess Gibbs energy functions of the binary phases of U-Zr system based on this data, using Lukas program, are given in table 11.

In table 12, invariant compositions and temperatures calculated using excess Gibbs energy functions listed in table 11, are compared with those given in assessed phase-diagram of Sheldon and Peterson [51], and calculated ones of Leibowitz et al. [26] and Ogawa and Iwai [27]. As can be seen that all the three sets of equilibrium are in reasonably good agreement with each other. Leibowitz et al. [26] and Ogawa and Iwai [27] have also calculated phase diagram of uranium-zirconium system by computer based analysis using thermodynamic models.

The calculated invariant points are in reasonably good agreement with assessed values of Sheldon and Peterson [51]. The U-Zr phase diagram based on present calculations is given in figure 10. A uranium rich partial phase diagram is given in figure 11. Present set of Gibbs energies show a decrease in transition temperature of $\beta\leftrightarrow\alpha$ with addition of zirconium, therefore, it is a eutectoid transition, $(\beta U)\leftrightarrow\varepsilon+(\alpha U)$. This is in agreement with most of the reliable experimental works reported, Zegler [47], Summer-Smith [49], Howlett and Knapton [59] etc. and contrary to the suggestion made by Lagerberg [61] that it should be a peritectoid reaction, $(\beta U)+\varepsilon\leftrightarrow(\alpha U)$, at slightly higher temperature than the $\alpha\leftrightarrow\beta$ transition temperature of pure uranium metal. The sub-solidus phase-boundary of $\varepsilon/((\beta U)+\varepsilon)$ is concave in shape, which is in better agreement with calculated phase boundary given by Leibowitz et al. [52] compared to convex phase boundary shown in the assessed phase diagram given by Sheldon and Peterson [51].

A zirconium rich partial phase diagram, comparing calculated phase boundaries of the compound κ-UZr_2 with experimental data is given in figure 12. As can be seen from this figure that the phase boundaries of κ-UZr_2 drawn based on present calculations are in better agreement with Howlett and Knapton [59] than the ones given by Duffey and Bruch [65]. The later has indicated a much narrower range of non-stoichiometry of the compound. In figure 13, liquidus-solidus equilibrium

calculated using present set of Gibbs energy values is compared with literature data. The solidus and liquidus temperatures given by Kanno et al. [76], based on their partial Gibbs energy data, are lower than that of Massalski et al.[75], but are in reasonable agreement with present liquidus-solidus curves.

As shown in figure 14, the partial Gibbs energy values of uranium given by Fedorov and Smirnov [63] are more negative than the one calculated from the optimized Gibbs energy of (ε-U,Zr) given in table 11. Fedorov and Smirnov have reported a minimum Gibbs energy of mixing of –12 kJ/mol at 1073 K and approximately 70 at.% Zr. Whereas, Gibbs energy of mixing calculated from present set of optimized data, was –1.45 kJ/mol, at the same temperature and composition. This value is less negative than the ideal Gibbs energy of mixing, which can explain the presence of miscibility gap in the system near this temperature. The Gibbs energy of mixing of (ε-U,Zr), calculated using the Gibbs energy functions given by Leibowitz et al. [52] and Pelton et al. [82], were also found to be much higher than that of Fedorov and Smirnov [63]. But unlike our values which show a minimum in Gibbs energy vs composition curve at approximately, 45 at% Zr, their data shows a minimum at approximately 65 at.% Zr (–3.5 kJ/mol). As seen from figure 15, experimentally determined integral Gibbs energy of mixing of U-Zr alloys reported by Kanno et al. [76], at 1773 K, is more negative than the ones calculated from optimized Gibbs energy functions given by Leibowitz et al., Pelton et al. and obtained during present calculations. However, Gibbs energy values calculated using present Gibbs energy function shows a minimum in zirconium rich alloys, which is in agreement with the observation made by Kanno et al. [76]. Which indicates that U-Zr liquid alloys are quite stable in the uranium-rich composition region. But the Gibbs energy of mixing values calculated using Leibowitz et al. and Pelton et al. [82] Gibbs energy functions were found to show a minimum near, ~55 at.% Zr. As shown in figure 16, the experimentally determined uranium activity values by Ohmichi [77], taken from Ogawa and Iwai [27], are in better agreement with present calculations compared to that of Leibowitz et al. [26,52] and Pelton et al. [82].

In figure 17, experimentally determined heat capacities of κ-UZr_2 compound are compared with calculated values. Takahashi et al. values indicate a sudden change in slope at approximately 600 K, otherwise their values are in reasonable agreement with present calculations. Heat capacity values of Fedorov and Smirnov [63] are much higher than the calculated values. A curve is drawn for estimated heat capacity using Neumann-Kopp's additivity rule. As commented by Takahashi et al. [83], who measured thermal diffusivity of U-Zr alloys, Newmann Kopps approximation should be closer to the heat capacity of U-Zr alloys than the values given by Fedorov and Smirnov. Heat capacity of δ-phase, calculated using present Gibbs energy equation is lower than that obtained by Newmann Kopps rule. This is in agreement with Takahashi et al. [83] thermal diffusivity measurements, where they observed that the κ-UZr_2 compound with 72 at.% zirconium shows minimum thermal diffusivity compared to all other alloy compositions studied by them. The calculated enthalpy of formation of the intermetallic compound κ, -1.2 kJ/mol for 67 at.% Zr, is within the reported experimental error bar value of enthalpy of formation given by Nagrajan et al. [81].

2.4. Plutonium-uranium-zirconium

The ternary system Pu-U-Zr is assumed to be comprised of binary phases with most of them showing solubility for all the three components. However, Pu(α) is assumed to be a pure binary phase

(Pu-Zr), with limited solubility of zirconium but negligible solubility of uranium. The binary intermetallic compound of Pu-Zr, ξ, was assumed to be stoichiometric compound during calculation of the binary system. Even during the calculations of the ternary Pu-U-Zr system, this compound was assumed to be a stoichiometric binary compound with no solubility of uranium. Other binary intermetallic compounds of Pu-Zr system, θ and ι, were also assumed to be pure binary compounds with no solubility of uranium. The only intermetallic compound of Pu-Zr, which was considered to be stable in ternary system with considerable uranium solubility, was κ. Ellinger and Land [28] and Lauthier et al. [41] have shown their doubts on the stability of this compound in Pu-Zr system, contrary to the reported work of Marples [29] and Bochvar et al. [9]. But analysis of the ternary Pu-U-Zr alloy systems by O'Boyle and Dwight [42] have clearly indicated stabilization of UZr_2 intermetallic in the ternary system by dissolution of plutonium. This is agreement with Marples [29] analysis that the structure of $PuZr_3$ is similar to that of δ-UZr_2. However, O'Boyle and Dwight [42] have reported that the unit cell constants of $PuZr_2$ as reported by Bochvar et al. [9] are in better agreement with the extrapolated ternary data than that of $PuZr_3$. Considering this ternary data, Pu-Zr binary was calculated with $PuZr_2$, reported by Bochvar et al. [9], instead of $PuZr_3$, reported by Marples [29]. The three binary liquid phases Pu-U, Pu-Zr and U-Zr were assumed to be completely soluble in each other. Similarly, the three binary solid solutions, ε-(Pu(ε),U(γ)), ε-(U(γ),Zr(β)) and ε-(Pu(ε),Zr(β)), were considered completely soluble in each other. This ternary solid solution is expressed as ε-(Pu(ε),U(γ),Zr(β)) in further discussions. O'Boyle and Dwight [42] have reported a limited solubility of zirconium in high temperature intermetallic of Pu-U, η. Whereas, they report up to 5% solubility of zirconium in the low temperature intermetallic of Pu-U, ζ. Therefore, these phases were also considered to contain all the three constituent elements, i.e., plutonium, uranium and zirconium. Other than Pu(α), all other allotropes of plutonium, uranium and zirconium were considered to dissolve other elements to some extent based on their solubility limits in the binary systems.

The Gibbs energy functions of Pu-U-Zr system were calculated using the Gibbs energy functions of the binary phases of the systems Pu-U, Pu-Zr and U-Zr, as discussed in previous sections. Very limited experimental data is available on phase diagram analysis of Pu-U-Zr ternary system [26], [42] and [84]. The Gibbs energy function of ternary solution phases consists of three parts, (i) phase stabilities of the elements, (ii) Redlich- Kister coefficients obtained during binary calculations in the order, Pu-U, Pu-Zr and U-Zr and (iii) excess Gibbs energy, if any, due to ternary mixing. In present calculations, the binary polynomial terms were extrapolated into the ternary system by Muggianu's formula [85]. Therefore, the last term was expressed by Muggianu's formula in which all the three elements of the solution are treated alike. The Gibbs energy of the ternary solution phases can be expressed as follows:

$$G_{ter} = \sum x_i G_i + RT\sum x_i \ln(x_i) + (x_{Pu\text{-}U} G^{ex}_{Pu-U} + x_{Pu\text{-}Zr} G^{ex}_{Pu-ZR} + x_{U\text{-}Zr} G^{ex}_{U-Zr}) + x_{Pu} x_U x_{Zr} K. \quad (10)$$

Where, the last term in the equation is ternary excess Gibbs energy part in which K is an SGTE function of temperature as given in equation (1). G^{ex}_{Pu-U}, G^{ex}_{Pu-Zr} and G^{ex}_{U-Zr} are excess Gibbs energy terms of binary solutions, calculated during optimization of the binary systems.

Leibowitz et al. [26] have calculated the excess Gibbs energies of the ternary liquid and solid solutions from the three binary systems using Kohler interpolation method:

$$G^{ex}_{ter} = (1\text{-}x_{Pu})^2 G^{ex}_{U-Zr} + (1\text{-}x_U)^2 G^{ex}_{Pu-Zr} + (1\text{-}x_{Zr})^2 G^{ex}_{Pu-U}$$

Where, G^{ex}_{U-Zr}, G^{ex}_{Pu-Zr} and G^{ex}_{Pu-U} are the excess Gibbs energies calculated for the binaries for the same compositional ratios, x_U/x_{Zr}, x_{Pu}/x_{Zr} and z_{Pu}/x_U as that of the ternary composition. In their calculations, Leibowitz et al. [26] have assumed ideal liquid solution and non-ideal solid solution for Pu-U and Pu-Zr binary systems, whereas, excess Gibbs energies of mixing are given for liquid and solid solutions of U-Zr. They have calculated liquidus and solidus temperatures using this model, which are given in a diagram. But for certain compositions, they have given calculated liquidus-solidus temperatures for comparison with experimental data. A comparison of their experimental liquidus-solidus temperatures of U-Zr system with literature data indicated some discrepancies. Even in their later publication, Leibowitz et al. [52] have reported different excess Gibbs energy expressions for liquid and solid-solution of U-Zr system than given during the calculations of the U-Pu-Zr ternary system. The later publication of Leibowitz et al. [52] is a simultaneous calculation of all the phases of U-Zr system, unlike their previous publication where only liquid and solid-solution phases were calculated. In the later publication [52], they argued that the new Gibbs energy functions also gave the liquidus-solidus similar to that of their previous optimization. But it should be noticed that for U-Zr binary with 19.3 at% Zr, the experimental liquidus and solidus temperatures reported by Leibowitz et al. [26] are, 1631 K and 1489 K, respectively, which are lower than their calculated values, 1644 K and 1494 K. However, calculations based on the Gibbs energy values given in their later publication [52], gave the liquidus and solidus temperatures, 1608 K and 1542 K respectively. During present optimization calculations of U-Zr system, it was observed that increase in weightage of liquidus-solidus data to get better fitting for these data, considerably increased the critical temperature of the miscibility gap of (ε-U,Zr) phase. Hence, the weightage to the experimental liquidus-solidus data was given according to the reported experimental error. The calculated liquidus and solidus temperatures calculated from the U-Zr excess Gibbs energy coefficients given in table 11 are, 1584 and 1515 K, respectively, for 19.3 at% Zr. This considerable difference in the experimental values reported for U-Zr binary [26] and present values is carried over to the ternary liquidus-solidus temperatures, as seen in table 13. Another set of experimental data for liquidus-solidus temperatures from MLM report [43] is also compared with present calculations. The difference in measured liquidus and solidus temperatures are reasonably high compared to calculated values. However, it is generally observed that the difference in the experimental liquidus and solidus temperatures is more reliable than the liquidus and solidus temperatures themselves as many of the experimental errors get cancelled while calculating the difference. As can be seen from the values given in table 13, values of $T_{liquidus}$-$T_{solidus}$, of the liquidus-solidus temperatures given by MLM report [43] are in very good agreement with present calculations. The liquidus and solidus surfaces of Pu-U-Zr ternary system at different temperatures, calculated using the above method are given in figure 18. The compositions for which experimental liquidus-solidus data are available in literature and are compared in table 13 with calculated values, are marked in the figure. As seen from the figure, these are all uranium rich alloys which are of interest for nuclear fuel.

O'Boyle and Dwight have analysed thirteen different compositions of U-Pu-Zr system by electron-microprobe analysis, x-ray diffraction and optical metallography techniques. All these compositions are closer to U-Zr binary with less than 50 at.% plutonium. The x-ray diffraction technique was used by them to study four ternary alloys near ζ intermetallic of Pu-U and six ternary

alloys near the δ intermetallic compound of U-Zr. They determined the ε-(Pu(ε),U(γ),Zr(β)) solvus by electron microprobe analysis. It is very difficult to assess the compositions of the alloys studied by them as they are given in a small figure. However, the main features of their work are: (i) a miscibility gap in ε-(Pu(ε),U(γ),Zr(β)), shown as ε' and ε'', uranium rich and zirconium rich solid-solution phases, formed by a monotectoid reaction in the U-Zr binary. In the binary system, U-Zr, this miscibility gap disappears below 966 K, as the uranium rich solid-solution decomposes into U(β) and zirconium rich solid-solution. However, in ternary system, O'Boyle and Dwight [42] have shown this miscibility gap in an isothermal section at 933 K. This indicates that the uranium rich solid-solution phase is stabilised to lower temperatures by addition of plutonium. The miscibility gap extends into the ternary system to ~17 at.% Pu. As the temperature decreases, the ε-(Pu(ε),U(γ),Zr(β)) solvus moves away from U-Zr binary, rapidly towards the central region, (ii) U(α) and U(β) dissolve up to 15 at.% and 20 at.% plutonium, respectively, but very limited amount of zirconium, (iii) Eta (η), the high temperature intermetallic of Pu-U, dissolves limited amount of zirconium, whereas, the low temperature intermetallic of Pu-U system, zeta (ζ) dissolves up to 5 at.% of zirconium. But O'Boyle and Dwight have not given any definite data for these solubility limits and respective temperatures, (iv) Kappa (κ), a U-Zr intermetallic shows an extensive solubility for plutonium and (v) Pu(δ), an FCC allotrope of plutonium shows extensive solubility for zirconium but very limited solubility for uranium.

In the absence of sufficient experimental data, it is difficult to determine a reliable Scheil-Scheme. As reported by O'Boyle and Dwight [42], a limited amount of zirconium is soluble in both binary intermetallics of Pu-U, ζ and η. But they have not given any quantitative data, which can be used for optimization of ternary ζ and η intermetallics. Calculations based on only binary excess Gibbs energy functions for these two compounds did not give us the reaction scheme given by O'Boyle and Dwight. In binary Pu-U system, the highest temperature at which the intermetallic compound ζ is formed is 546.5 K by the reaction, $\eta \leftrightarrow \zeta + (\beta Pu)$. Whereas, O'Boyle and Dwight have shown presence of ζ-compound at 943 K. It is possible only due to stabilisation of this compound in the ternary system by dissolution of zirconium. Similar to the reported observation of O'Boyle and Dwight, present calculations also indicated stabilisation of ε-(Pu(ε),U(γ),Zr(β)), ternary solid-solution, to low temperature compared to binary solid-solutions. This phase is of great importance for nuclear fuel. An isothermal section of the ternary phase diagram at 980 K calculated using present Gibbs energy values is given in figure 19. Savage [24] has reported enthalpy increment values of $Pu_{0.13}U_{0.65}Zr_{0.22}$ ternary alloy, in the temperature range 298-1413 K, using by drop calorimetry. Unlike the binary alloy, $Pu_{0.1}U_{0.9}$, which shows three transitions in the same temperature range, the ternary alloy shows either one transition at approximately 873 K or two transitions in the temperature range 873-973 K.

It was observed that the axial growth of irradiated Pu-U-Zr fuel in the reactor depends significantly on plutonium content [86]. The axial growth was found to be less than 6% when plutonium content of Pu-U-Zr was more than 17 at.%. This may be due to stabilisation of the BCC structured ε solid-solution with addition of plutonium, even at lower temperatures. In EBR-II, $U_{0.78-x}Pu_xZr_{0.22}$ (x = 0, 0.03, 0.07, 0.16, 0.19, 0.22, 0.24) alloy fuel has been tested with variety of cladding materials. The fuel showed excellent performance up to 10 at.% burn up. As reported in Kurata et al. [87], during irradiation, a significant redistribution of elements takes place due to temperature gradient. Previous irradiation studies by Murphy et al. [88] and Pahl et al. [89, 90] showed a significant migration of zirconium to the centre, a high temperature zone, and to the surface, a cold temperature zone. Whereas,

uranium was observed to move both from centre and surface zones to the intermediate zone. On the contrary, out of pile experiments by Harbur et al. [84] and Porter et al. [91] showed that zirconium moved mainly from the centre towards the outer region, whereas, uranium moves in the opposite direction, with plutonium enrichment in the intermediate region. Tsai and Neimark [92] also observed plutonium enrichment in the intermediate region by α-autoradiography. These discrepancies in the migration behaviour of the elements observed by various researchers may be due to the temperature differences of their samples. From the knowledge of phase equilibria, it can be inferred that when the centreline temperature is near 940 K, the ternary alloy of composition $Pu_{0.16}U_{0.61}Zr_{0.22}$ exists as zirconium rich and zirconium deficient solid-solutions, ε+ε'. At lower temperatures, zirconium deficient solid-solution gets converted into ε+ζ. It should be noticed that the tetragonal, Pu-U binary intermetallic compound, ζ, is never in equilibrium with BCC, (ε-Pu,U) solid-solution. In the binary system, it is formed on cooling of high temperature intermetallic compound, η, which is also a tetragonal compound. But in ternary system, ζ gets stabilised by addition of zirconium to the extent that it is not only stable at temperatures higher than those in Pu-U binary but it is also in equilibrium with ε-(Pu(ε),U(γ),Zr(β)) solid-solution over most of the composition and temperature range. In binary system, the highest temperature at which ζ intermetallic appears is 863 K, whereas, in ternary it is formed at 943 K. On cooling, the zirconium rich solid-solution, ε-(Pu(ε),U(γ),Zr(β)), gets converted in ε+δ. Both ε+δ and ε+ζ, on further cooling get converted into ζ+δ phase field. The intermetallic compound ζ is identified as a complex cubic structure by O'Boyle and Dwight [42], whereas, on extensive X-ray diffraction analysis of the compound at high temperature and room temperature, Ellinger et al. [10] concluded that ζ may have a tetragonal lattice with an axial ratio of unity at room temperature, which explains anisotropic expansion at high temperature and cubic lattice at room-temperature. As the lattice structures and lattice parameters of the two Pu-U intermetallics, η and ζ have very little difference, therefore, it may be possible that the phase shown as ζ by O'Boyle and Dwight in Pu-U-Zr ternary was in fact η. In that case the whole Schiel scheme shown by O'Boyle and Dwight will change. Further experimental work is required to establish the presence of the compound ζ with ε-(Pu(ε),U(γ),Zr(β)) at temperatures above 863 K. A recent work reported by Kurata [93], based on thermodynamic and phase diagram parameters of Pu-U-Zr system, has given calculated ternary phase diagrams which are in reasonable agreement with experimentally reported work of O'Boyle and Dwight. However, he has assumed a limited solubility of Pu in UZr_2 intermetallic compound. However, according to O'Boyle and Dwight, Pu shows extensive solubility in UZr_2. Pu-Zr phase diagram given by Kurata shows only one intermetallic compound, θ, thus excluding all other intermetallic compounds of Pu-Zr system, ξ, ι and κ. Kurata has also shown a very composition range of stability for the compound θ, below 575 K. Further work needs to be carried out to be able to calculate Gibbs energy functions of ternary phases based on the sets of coefficients of the binary systems that define the binary systems completely and reliably.

References

[1] C.H. Till and Y.I. Chang, Proc. American Power Conference, Chicago, IL, 1986, p.688.
[2] Y.I. Chang, Nucl. Technology, 88(1989)129.
[3] G.L. Hofman, Nucl. Technology, 47(1980)7.
[4] H.L. Lukas, E.-Th. Henig and B. Zimmermann, Calphad 1 (1977) 225-236.
[5] H.L. Lukas, S.G. Fries, J. Phase Equilibria, 13 (1992) 532-541.
[6] O. Redlich, A. Kister, Indust. Eng. Chem. 40 (1948) 345-348.

[7] A.T. Dinsdale, Calphad 15 (1991) 317-425.
[8] L. Leibowitz, R.A. Blomquist and A.D. Pelton, J. Nucl. Mater., 184 (1991) 59-64.
[9] A.A. Bochvar, S.T. Konobeevskii, V.I. Kutaitsev, T.S. Menshikova and N.T. Chebotarev, Proc. 2nd U.N. Int. Conf. On Peaceful Uses of Atomic Energy, Vol. 6, United Nations, Geneva (1958) 184-193, A/CONF/15/P2197.
[10] F.H. Ellinger, R.O. Elliott and E.M. Cramer, J. Nucl. Mater. 3 (1959) 233-243.
[11] M.B. Waldron, The Metal Plutonium, A.S. Coffinberry and W.N. Miner, Ed., University of Chicago Press, Chicago (1961) 225-239.
[12] F.W. Schonfeld, The Metal Plutonium, A.S. Coffinberry and W.N. Miner, Ed., University of Chicago Press, Chicago (1961) 255-264.
[13] R.O. Elliott and A.C. Larson, The Metal Plutonium, A.S. Coffinberry and W.N. Miner, Ed., University of Chicago Press, Chicago (1961) 265-280.
[14] D.E. Peterson and E.M. Foltyn, Bull. Of Alloy Phase Diagrams, 10(2) (1989) 160-164
[15] A.F. Berndt, J. Nucl. Mater. 9(1) (1963) 53-58.
[16] A.S. Coffinberry, Second United Nations Conference of the Peaceful Uses of Atomic Energy, Geneva, 1958, A/Conf. 15/P/1046.
[17] Y. Okamoto, A. Maeda, Y. Suzuki and T. Ohmichi, J. Alloys and Compounds, 213/214 (1994) 372-374.
[18] Mound Laboratory Report MLM-1402 (1967).
[19] S. Rosen, M.V. Nevitt and J.J. Barker, J. Nucl. Mater. 9 (1963) 128.
[20] L.J. Wittenberg and G.R. Grove, Mound Laboratory Rep. MLM-1283 USAEC, Dayton, OH (1965).
[21] L.J. Wittenberg, D. Ofte, W.G. Rohr and D.V. Rigney, Metall. Trans., 2(1) (1971) 287-290.
[22] P. Chiotti, V.V. Akhachinskij, I. Ansara and M.H. Rand, The Chemical Thermodynamics of Actinide Elements and compounds. Part 5, The Actinide Binary Alloys, IAEA, Vienna, 254-257 (1981).
[23] H. Savage and R.D. Seibel, Argonne National Laboratory Report ANL-6702 (1963).
[24] H. Savage, J. Nucl. Mat., 25 (1968) 249-259.
[25] D.E. McKenzie, Can. J. Chem., 34 (1956) 515-522.
[26] L. Leibowitz, E. Veleckis, R.A. Blomquist and A.D. Pelton, J. Nucl. Mater. 154 (1988) pp. 145-153.
[27] T. Ogawa and T. Iwai, J. Less-Comm. Met., 170 (1991) 101-108.
[28] F.H. Ellinger and C.C. Land, Plutonium 1970 and other Actinides, W.N. Miner, Ed AIME, New York, 1970, p.686.
[29] J.A.C. Marples, J. Less-Common Metals, 2 (1960) 331-351.
[30] J.M. Taylor, J. Nucl. Mater., 30 (1969) pp. 346-350.
[31] Yasufumi Suzuki, Atsushi Maeda and Toshihiko Ohmichi, J. Alloys and Compounds, 182 (1992) L9-L14
[32] A.J. Perkins, A. Goldberg and T.B. Massalski, J. Nucl. Mater., 41 (1971) 39-50.
[33] A.S. Coffinberry and M.B. Waldron, Progress in Nuclear Energy, Vol. I, Pergamon Press, London and New York, 1956, Series V, Chapter 4.
[34] W.H. Zachariasen and F.H. Ellinger, USAEC Report LA-4391 Los Alamos Scientific Laboratory, 1970.
[35] V.I. Kutaitsev, N.T. Chebotarev, I.G. Lebedev, M.A. Anderianov, V.N. Konev and T.S. Menshikova, Plutonium 1965, A.E. Kay and M.B. Waldron (Eds) Chapman and Hall, London (1967) pp. 420-449.

[36] F.H. Ellinger, "Discussion of Plutonium, Zirconium Alloys", in Plutonium 1960, E. Grison, W.B.H. Lord and R.D. Fowler (Eds.), Cleaver-Hume Press Ltd, London (1961) pp. 318-319.
[37] F.H. Ellinger, W.N. Miner, D.R. O'Boyle and F.W. Schonfeld, LA-3870, Los Alamos Scientific Laboratory (1968).
[38] M.B. Waldron, J. Garstone, J.A. Lee, P.G. Mardon, J.A.C. Marples, D.M. Poole and G.K. Williamson, Proceedings of the Second United Nations International Conference on the Peaceful Uses of Atomic Energy, Geneva, 1958, A/Conf. 15/P/71.
[39] T.A. Sandenaw and D.R. Harbur, J. Chem. Thermodynamcis, 5 (1973) 459-465.
[40] J.M. Silcock, J. Nucl. Mater., 9 (1957) 521.
[41] J.C. Lauthier, N. Housseau, A. Van Craeynest and D. Calais, J. Nucl. Mat., 23 (1967) pp. 313-319.
[42] D.R. O'Boyle and A.E. Dwight, Plutonium 1970 and Other Actinides, ed. W.N. Miner (Metallurgical Society of AIME, New York, 1970), p 720.
[43] Mound Laboratory Report MLM-1346 (1967).
[44] F.A. Shunk, Constitution of Binary Alloys – Second Supplement, McGeaw-Hill, New York, 1969.
[45] A. Maeda, Y. Suzuki, Y. Okamoto and T. Ohmichi, J. Alloys and Compounds 205 (1994) 35-38.
[46] J.M. Sanchez and D. de Fontaine, Phys. Rev. Lett., 35 (1975) 227.
[47] S.T. Zegler and H.H. Chiswik, Nuclear Engineering and Science Conference, 11-14 March 1957, Paper No. 57-NESC-14
[48] H.A. Saller and F.A. Rough, Report No. BMI-1000, Office of Technical Services, Department of Commerce, Washington, D.C. (1955)
[49] D. Summers-Smith, J. Inst. Met., 83 (1954-55) 277-282.
[50] S.T. Zegler, "The Uranium-Rich End of the Uranium-Zirconium System," USAEC Rep. ANL-6055(1962).
[51] R.I. Sheldon and D.E. Peterson, Bulletin of Alloy Phase Diagrams, Vol.10, No. 2 (1989)165-171.
[52] L. Leibowitz, R.A. Blomquist and A.D. Pelton, J. Nucl. Mat., 167 (1989) 76-81.
[53] H.H. Chiswik, A.E. Dwight, L.T. Lloyd, M.V.Nevitt and S.T. Zegler, Second Geneva Conf., 15/P/713 (1958).
[54] F.A. Rough and A.A. Bauer, Constitutional Diagrams of Uranium and Thorium Alloys, Addison-Wesley Publ. Co., Reading, Mass. (1958).
[55] R.K. McGeary, U.S. At. Energy Comm. TID-5061, 1951 (declassified 1958), 419-437.
[56] F.A. Rough, A.E. Austin, A.A. Bauer and J.R. Doig, BMI-1092 (1956).
[57] A.A. Bauer, G.H. Beatty and F.A. Rough, Transactions of the American Society of AIME, 212 (1958) 801-808.
[58] J. Philibert and Y. Adda, Colloque sur la diffusion a l'etat Solide (North-Holland, Amsterdam, 1959) p.163.
[59] B.W. Howlett and A.G. Knapton, Proc. 2nd U.N. Int. Conf. On Peaceful Uses of Atomic Energy, United Nations Publication, Geneva, Volume 6, 1958, 104-110.
[60] R.L. Craik, D. Birch, C. Fizzotti and F. Saraceno, J. Nucl. Mater., 6 (1962) 13-25.
[61] G. Lagerberg, J. Nucl. Mater., 9 (1963) 261-276.
[62] A. Virot, J. Nucl. Mater., 5 (1962) 109-119.
[63] G.B. Fedorov and E.A. Smirnov, Atomnaya Energiya, 25 (1), (1968) 54-56.
[64] N. Mueller, Z. Metallkunde, 50 (1959) 562.
[65] J.F. Duffey and C.A. Bruch, Transactions of The Metalurgical Society of AIME, February (1958)17-19.

[66] A.N. Holden and W.E. Seymour, Trans. AIME, 206 (1956) 1312-1316.
[67] E.R. Boyko, Acta Crystallogr., 10 (1957) 712-713.
[68] M.H. Muller, H.W. Knott and L.R. Heaton, Abstract of paper presented at Pittsburgh Diffraction Conference, 6-8 November 1957.
[69] R.D. Barnard, Proc. Phys. Soc. (London), 78 (1961) 722-727.
[70] E.S. Makarov, Kristallografiya, 3 (1958) 5-9.
[71] A.A. Bauer, BMI-1350 (1959).
[72] M. Akabori, A. Itoh, T. Ogawa, F. Kabayashi and Y. Suzuki, J. Nucl. Mat. 188 (1992) 249-254.
[73] O.S. Ivanov and G.N. Bagrov, in 'Stroenie Splavov Nekotorykh Sistem c Uranom I Torien', Gosatomizdat, Moscow (1961) 5-19.
[74] L.G. Wisnyi and S. Pijanowski, U.S. At. Energy Comm. KAPL-1564 (1956) 45.
[75] T.B. Masasalski, Acta Met. 6 (1958) 243.
[76] M. Kanno, M. Yamawaki, T. Koyama and N. Morioka, J. Nucl. Mater., 154 (1988) 154-160.
[77] T. Omichi, (values taken from T. Ogawa and T. Iwai, J. Less-Comm. Met., 170 (1991) 101-108.
[78] G.B. Fedorov and E.A. Smirnov, Atomnaya Energiya, 21 (3), (1966) 189-192.
[79] A. Maeda, Y. Suzuki and T. Ohmichi, J. alloys and Compounds, 179 (1992) L21-L24
[80] Y. Takahashi, K. Yamamoto, T. Ohsato, H. Shimada and M. Yamawaki, J. Nucl. Mater., 167 (1989) 147-151.
[81] K. Nagrajan, R. Babu and C.K. Mathews, J. Nucl. Mater., 203(1993) 221-223.
[82] A.D. Pelton, P.K. Talley, L. Leibowitz and R.A. Blomquist, J. Nucl. Mater. 210 (1994) 324-332.
[83] Y. Takahashi, M. Yamawaki and K. Yamamoto, J. Nucl. Mater., 154 (1988) 141-144.
[84] D.R. Harbur, J.W. Anderson and W.J. Mariman, Los Alamos National Laboratory Report, LA-4512 (1970)
[85] Y.M. Muggianu, M. Gambino and J.P. Bros, J. Chim Physi., 72 (1975) 83.
[86] C.E. Lahm, J.F. Koenig, R.G. Pahl, D.L. Porter and D.C. Crawford, J. Nucl. Mat. 204 (1993) 119-123.
[87] M. Kurata, T. Inoue and C. Sari, J. Nucl. Mat., 208 (1994) 144-158
[88] W.F. Murphy, W.N. Beck, F.L. Brown, B.J. Koprowski and L.A. Neimark, USAEC Report, Argonne National Laboratory, ANL-7602 (1969)
[89] R.G. Pahl, C.E. Lahm, R. Villareal, W.N. Beck and G.L. Hofman, Proc. Int. Conf. On Reliable Fuels for Liquid Metal Reactors, Tucson, AZ, 1986, session 3, p. 36.
[90] R.G. Pahl, R.S. Wisner, M.C. Billone and G.L. Hofman, Proc. Int. Fast Reactor Safety Meeting, Snowbird, 1990, Session 2, p. 129.
[91] D.L. Porter, C.E. Lahm and R.G. Pahl, Met. Trans. A, 21A (1990) 1871-1876.
[92] H. Tasai and L.A. Neimark, Proc. Int. Conf. On Design and Safety of Advanced Nuclear Power Plants, Tokyo, Japan, 1992, Vol III, Session 28, p. 2.
[93] M. Kurata, Claphad, 23(3-4) (1999) 305-337.
[94] T. Matsui, T. Natsume, and K. Naito, J. of Nucl. Mater., 167 (1989) 152-159.
[95] M. Kurata, T. Ogata, K. Nakamura and T. Ogawa, J. Alloys and Compounds, 271-273 (1998) 636-740.

Table 1. The Gibbs energies of transitions of stable and hypothetical allotropes of plutonium from plutonium (α).

Phase transition	A	BT	CTln(T)
G^{l}_{Pu} -G^{α}_{Pu}	3534.24	35.18451	-6.694
G^{ε}_{Pu} -G^{α}_{Pu}	6822.85	-14.0528	0.0
$G^{\delta'}_{Pu}$ -G^{α}_{Pu}	4981.89	-11.61771	0.0
G^{δ}_{Pu} -G^{α}_{Pu}	4897.79	-11.50349	0.0
G^{γ}_{Pu} -G^{α}_{Pu}	4184.84	-10.301	0.0
G^{β}_{Pu} -G^{α}_{Pu}	3707.02	-9.32195	0.0
G^{η}_{Pu} -G^{α}_{Pu} (Pu-U)	6115.75	-12.91726	0.0
G^{ζ}_{Pu} -G^{α}_{Pu} (Pu-U)	4023.75	-6.55758	0.0

Table 2. The Gibbs energies of transitions of stable and hypothetical allotropes of uranium from uranium(α).

Phase transition	A	BT	CTln(T)
G^{l}_{U} -G^{α}_{U}	2112.92	71.57569	-10.376
G^{γ}_{U} -G^{α}_{U}	7547.94	-7.49773	0.0
G^{β}_{U} -G^{α}_{U}	2790.73	-2.96230	0.0
G^{η}_{U} -G^{α}_{U} (Pu-U)	3326.28	-3.31373	0.0
G^{ζ}_{U} -G^{α}_{U} (Pu-U)	2949.72	0.0	0.0
G^{κ}_{U} -G^{α}_{U} (U-Zr) Ogawa and Iwai [27]	527.00	0.0	0.0

Table 3. Phase diagram and thermodynamic data reported for Pu-U binary system.

Techniques	Range	Ref
Phase Diagram Data		
Assessed	Complete	Peterson and Foltyn [14]
Assessed	Complete	Leibowitz et al. [8]
Compiled	Liquidus↔(ε-Pu,γ-U)	Chiotti et al. [22]
DTA, Dilatometry, Metallography, XRD	Complete	Waldron [11]
Not given	Complete	Bochvar et al. [9]
XRD, Thermal Analysis and Optical Metallography	Complete	Schonfeld [12]
Thermal Analysis	Complete	Okamoto et al. [17]
Debye Scherrer Method	(αU) Solubility Range	Berndt [15]
Experimental	Liquid↔(ε-Pu,γ-U)	Mound Laboratory Report [18]
Experimental	Minimum in liquid+(ε-Pu,γ-U)	Rosen et al. [19], Wittenberg and Grove [20], Wittenberg et al. [21]
XRD, Dilatometry, DTA	Complete	Ellinger et al. [10]
XRD	Lattice Structure of ζ	Coffinberry [16]
Thermodynamic Data		
$\Delta H_{(T-298.15\ K)}$ of $(Pu_{0.1}U_{0.9})$ by isothermal drop calorimeter	T=298.15-1473 K	Savage and Seibel [23] Savage [24]
Vapor pressure over (Pu,U) liquid solution	T=1813-2042 K	McKenzie [25]

Table 4. Excess Gibbs energy functions of the Pu-U binary phases.

Binary Phases	Gibbs energy coefficients	A	BT
Liquid	x(1-x)	0.0	0.0
ε-(Pu(ε),U(γ))	x(1-x) x(1-x)(1-2x)	2997.41 -315.50	0.0 0.0
η	x(1-x) x(1-x)(1-2x) $x(1-x)(1-2x)^3$	-2333.88 -8954.36 -704.58	5.54765 9.84271 1.96909
ζ	x(1-x) x(1-x)(1-2x) $x(1-x)(1-2x)^3$	-18366.96 766.68 7852.78	12.54438 2.90019 -20.01413
(αPu)	x(1-x)	0.0	0.0
(βPu)	x(1-x)	6193.04	0.0
(γPu)	x(1-x)	8870.09	0.0
(δPu)	x(1-x)	8876.30	0.0
(δ'Pu)	x(1-x)	8726.16	0.0
(αU)	x(1-x)	1399.38	-1.85233
(βU)	x(1-x)	4849.73	-2.61174

Table 5. Calculated invariant temperatures and compositions for Pu-U system.

Equilibrium Reactions	Present Calculations		Peterson and Foltyn [14]		Leibowitz et al. [8]	
	T (K)	at.% U	T.(K)	at.% U	T(K)	at.% U
(ε-Pu,U)↔liquid (Liq.-Sol. Minimum)	903	12.0			899	~0.1
(ε-Pu,U)↔(δ'Pu)+η (Eutectoid)	724.6	2.6, 1.4, 4.5	728	2.5, 1.3, 4.5	727	2.5, 1.1, 4.3
(δ'Pu)↔(δPu)+η (Eutectoid)	717.6	1.44, 1.4, 4.7	715	1.2, 0.3, 4	710	1.1, 1.2, 5
η+(δPu)↔(γPu) (Peritectoid)	593.0	8.1, 1.6, 1.6	593	2.0, 0.2, 0.25	591	9, 1.8, 1.8
(γPu)+η↔(βPu) (Peritectoid)	553.6	1.7, 10.1, 3.2	553	0.8, 2.6, 2.0	555	1.9, 11.5, 3
η↔ζ+(βPu) (Eutectoid)	546.5	10.6, 24.1, 3.3	551	2.7, 25.0, 2.0	551	12.0, 25, 3.1
(βPu)↔(αPu)+ζ (Peritectoid)	394.6	0.9, 0.0, 23.8	398	0.1, 0.15, 29.5	394	1, 0.0, 25
(ε-Pu,U)+(βU)↔η (Peritectoid)	978.2	71.2, 75.5, 72.5	978	70.0, 80.0, 70.5	975	71, 76, 72.5
(βU)+η↔ζ (Peritectoid)	862.7	72.6, 67.8, 70.2	863	82.0, 67.5, 72.0	859	81, 79, 75
(βU)↔(αU)+ζ (Eutectoid)	833.3	81.3, 86.3, 74.3	833	83.0, 85.0, 74.0	830	85.0, 90.0, 78.0

- **Where, (ε-Pu,U) represent ε-(Pu(ε),U(γ))**

Table 6. The Gibbs energies of transitions of stable and hypothetical allotropes of zirconium from zirconium(α).

Phase transition	A	B×T	C×T×ln(T)
G^{l}_{Zr}-G^{α}_{Zr}	24870.00	-13.315	0.0
G^{β}_{Zr}-G^{α}_{Zr}	3940.0	-3.475	0.0
G^{κ}_{Zr}-G^{α}_{Zr} (Pu-Zr) and (U-Zr) Sanchez and de Fontaine [46]	846.0	-	-

Table 7. Phase diagram and thermodynamic data reported for Pu-Zr binary system.

Techniques	Range	Ref
Phase Diagram Data		
Assessment	Complete	Kurata [93]
Compilation	Liquidus-Solidus	Shunk [44]
Assessment	Liquidus-Solidus	Leibowitz et al. [26]
XRD, Dilatometry, DTA	Complete	Marples [29]
DTA, Dilatometry, Metallography, XRD	Complete	Waldron [11]
DTA, Dilatometry, Micrography, XRD	Complete	Ellinger and Land [28]
XRD, Thermal Analysis and Optical Metallography	Complete	Schonfeld [12]
DTA and XRD	> 50 at.% Zr	Suzuki et al. [31]
XRD and Metallography	≤10 at.% Zr	Taylor [30]
Not given	Complete	Bochvar et al. [9]
DTA, XRD, Metallography, Dilatometry	2-14 at.% Zr	Kutaitsev et al. [35]
Metallography, XRD	5-45 at.% Zr	Perkin et al. [32]
Thermodynamic Data		
Partial vapour pressure of plutonium over (Pu,Zr) alloys by Quadrupole Mass-spectrometer	T=1400-1900 K, X=20,50,60,75,82 and 94 at.% Zr	Maeda et al. [45]
Cp of ξ	T=15-373 K X=2.55 at.% Zr	Sandenaw and Harbur [39]

Table 8. Excess Gibbs energy functions of the Pu-Zr binary phases.

Binary Phases	Gibbs energy coefficients	A	B	C
Liquid	x(1-x)	0.0	0.0	
(ε-Pu,Zr)	x(1-x)	5204.89	0.67574	
κ	x(1-x) x(1-x)(1-2x) $x(1-x)(1-2x)^2$	2185.21 33824.56 46269.70	3.62761	
θ	x(1-x) x(1-x)(1-2x) $x(1-x)(1-2x)^2$	-61533.79 178512.20 -160209.96	5.21068 0.0 0.0	
ι	x(1-x) x(1-x)(1-2x) $x(1-x)(1-2x)^2$	11864.23 -54442.77 24620.05	5.31908 0.0 0.0	
ξ		-3114.77	38.61948	-5.815184
(αPu)	x(1-x)	-126549.27	284.22886	
(βPu)	x(1-x)	-123909.69	217.84019	
(γPu)	x(1-x)	-89795.55	159.11241	
(δPu)	x(1-x) x(1-x)(1-2x) $x(1-x)(1-2x)^2$	-3159.81 1637.35 -10532.44 -31254.40	10.61821 -5.27463 19.27731 42.69838	
(δ'Pu)	x(1-x)	6970.25	0.0	
(αZr)	x(1-x) x(1-x)(1-2x)	14811.92 20026.86	2.31859 0.0	

Table 9. Calculated temperatures and compositions at invariant points of Pu-Zr system.

Equilibrium Reactions	Present Calculation		Ellinger and Land [28]		Marples [29]	
	T(K)	at.% Zr	T(K)	at.% Zr	T(K)	Reaction & at.% Zr
(ε-Pu,Zr)↔(αZr)+(δPu) Eutectoid	890.0	69.6, 88.9, 68.6	894	~70.0, ~87, ~70	891	Same Reaction 73, 87, 70
(δPu)+(ε-Pu,Zr)↔(δ'Pu) Peritectoid	758.0	5.1, 4.3, 4.4	-	-	758	Same Reaction 5, 2, 2.5
(αZr)+(δPu)↔κ Peritectoid	652.95	88.7, 65.8, 69.2	-	-	653	89, 64, 74
(δPu)+ι↔θ Peritectoid	584.2	12.85, 19.2, 14.9	587	~14, 20, ~14	-	-
(δPu)+(γPu)↔ξ Peritectoid	544.8	2.72, 2.24, 2.7	545±3	4, 1.5, 3.4	553	(δPu)↔(γPu)+θ 2.6,2.5,12
(δPu)↔θ+ξ Eutectoid	542.0	4.0, 8.06, 2.7	541	4, 6, 3.4	-	-
(δPu)↔ι+κ Eutectoid	539.4	53.1, 24.4, 65.8	-	-	540	(δPu)↔θ+κ 55,25,74
(γPu)+ξ↔(βPu) Peritectoid	528.61	0.914, 2.7, 1.76	-	-	533	(γPu)+θ↔(βPu) 2.5, 12, 6
(βPu)↔(αPu)+ξ Eutectoid	397.18	0.134, 0.0, 2.7	-	-	388	(βPu)↔(αPu)+θ 3, 2, 11

Table 10. Phase diagram and thermodynamic data reported for U-Zr binary system.

Techniques	Range	Ref
Phase Diagram Data		
Assessed	Complete	Sheldon and Peterson [51]
Optimization	Liquidus-solidus	Pelton et al. [82]
Assessment and Optimization	Complete with no details	Kurata et al. [95]
Optimization	Complete	Leibowitz et al. [52]
Metallography, Dilatometry, XRD	Complete	Summers-Smith [49]
Metallography, XRD, TA	≤84.3 at.% Zr	Zegler [47]
Metallography, XRD	57-86 at.% Zr	Duffey and Bruch [65]
Microanalysis, XRD, DTA	18-95 at. % Zr	Akabori et al. [72]
TA, XRD, Electrical Resistance, Metallography	64, 73, 80 and 90 at.% Zr	Holden and Seymour [66]
DTA, Metallography	1.3, 5, 12.1 at.% Zr	Lagerberg [61]
Metallography	< 8.5 at.% Zr	Craik et al. [60]
Metallography, XRD,Dilatometry	50-90 at.% Zr	Howlett and Knapton [59]
Thermodynamic Data		
$\Delta \overline{G}_U$ of l(U,Zr) and (ε-U,Zr)	x_U=0.098-0.860 T=1700-2060 K	Kanno et al. [76]
$\Delta \overline{G}_U$ of (ε-U,Zr)	x_U=0.06-0.86 T=1023-1183 K	Fedorov and Smirnov [78]
Heat Capacity of κ and (ε-U,Zr)	14, 35, 72, 91 at.% Zr 300-1100 K	Takahashi et al. [80]
Heat capacity of κ	x_U=0.73 T=293-873 K	Fedorov and Smirnov [78]
Heat capacity of (ε-U,Zr)	997-1290 K x_U=0.8	Matsui et al. [94]
a_U in liquid and (ε-U,Zr)	24.4, 39.3 at.% Zr 1673-1873 K	Maeda et al. [79]

Table 11. Optimized excess Gibbs energies of U-Zr phases.

Binary Phases	Gibbs energy coefficients	A	B×T	C×T×ln(T)
Liquid	x(1-x) x(1-x)(1-2x)	112938.72 -21730.45	-64.50130 0.0	0.0 0.0
(ε-U,Zr)	x(1-x) x(1-x)(1-2x) $x(1-x)(1-2x)^2$	-1016173.73 24583.48 11841.12	920.47166 -23.33820 -7.68366	-115.223583 0.0 0.0
κ	x(1-x) x(1-x)(1-2x) $x(1-x)(1-2x)^3$	-2072.62 12812.79 5584.44	21.52422 -10.11506 0.0	0.0 0.0 0.0
(αU)	x(1-x)	39613.56	0.0	0.0
(βU)	x(1-x)	36485.22	0.0	0.0
(αZr)	x(1-x)	44436.83	0.0	0.0

Table 12. Comparison between present values with literature values of temperatures and compositions of the equilibrium phases at invariant points for U-Zr system

Equilibrium Reactions	Present Calculations		Ogawa and Iwai [27]		Sheldon and Peterson [51]		Leibowitz et al. [26]	
	at.% Zr	T (K)	at.% Zr	T (K)	at.% Zr	T (K)	at.% Zr	T (K)
(ε-U,Zr)↔(ε'-U,Zr)+(βU) (Monotectoid)	10.5,46.2, 1.0	964	9.7,47, 1.1	961	10.9,42.4, 1.1	966	11,42.5,1.1	965
(βU)→(αU)+(ε-U,Zr) (Eutectoid)	0.9,0.59, 57.7	934	~1.1,~1.0, 57	932	0.8,0.5, 60	935	0.8,0.5,58	928
(ε-U,Zr)+(αU)→κ (Peritectoid)	66.3,0.47, 63.1	891	68,0.5, 65	885	~66,~0.5, 63	890	~68,0.5,~68	889.6
(ε-U,Zr)→κ +(αZr) (Eutectoid)	79.1,77.5, 99.8	879	78,76, 99.6	883	~81,~78, 99.6	879	82,~74,99.6	880
(ε-U,Zr)↔(ε'-U,Zr)+(ε''-U,Zr) (Critical Temp.)	26	1003	30	995	~28	~995	~20	~1000

Table 13. Comparison of calculated (calc.) and experimentally determined (exp.) liquidus-solidus temperatures of Pu-U-Zr ternary.

Composition			Liquidus Temp. (K)					Solidus Temp. (K)				
x_{Pu}	x_U	x_{Zr}	Experimental			Calculated		Experimental			Calculated	
			[26]	[84]]	[42]	[26]	present	[26]	[84]	[42]	[26]	Present
0.195	0.772	0.033	1323	-		1333	1321	1069	-		1285	1250
0.193	0.662	0.145	1594	-		1489	1483	1366	-		1344	1354
0.13	0.71	0.16	-	1513		1541	1516	-	1378		1394	1404
0.12	0.59	0.29	-	1698		1667	1655	-	1468		1460	1519
0.85	0.1	0.05			1048		1098			948		989
0.8	0.1	0.1			1128		1202			983		1060
0.75	0.15	0.1			1138		1234			993		1074
0.7	0.2	0.1			1233		1262			1038		1088
0.7	0.15	0.15					1317			1078		1140
0.75	0.05	0.2					1314			1063		1155
0.7	0.05	0.25					1379			1148		1204

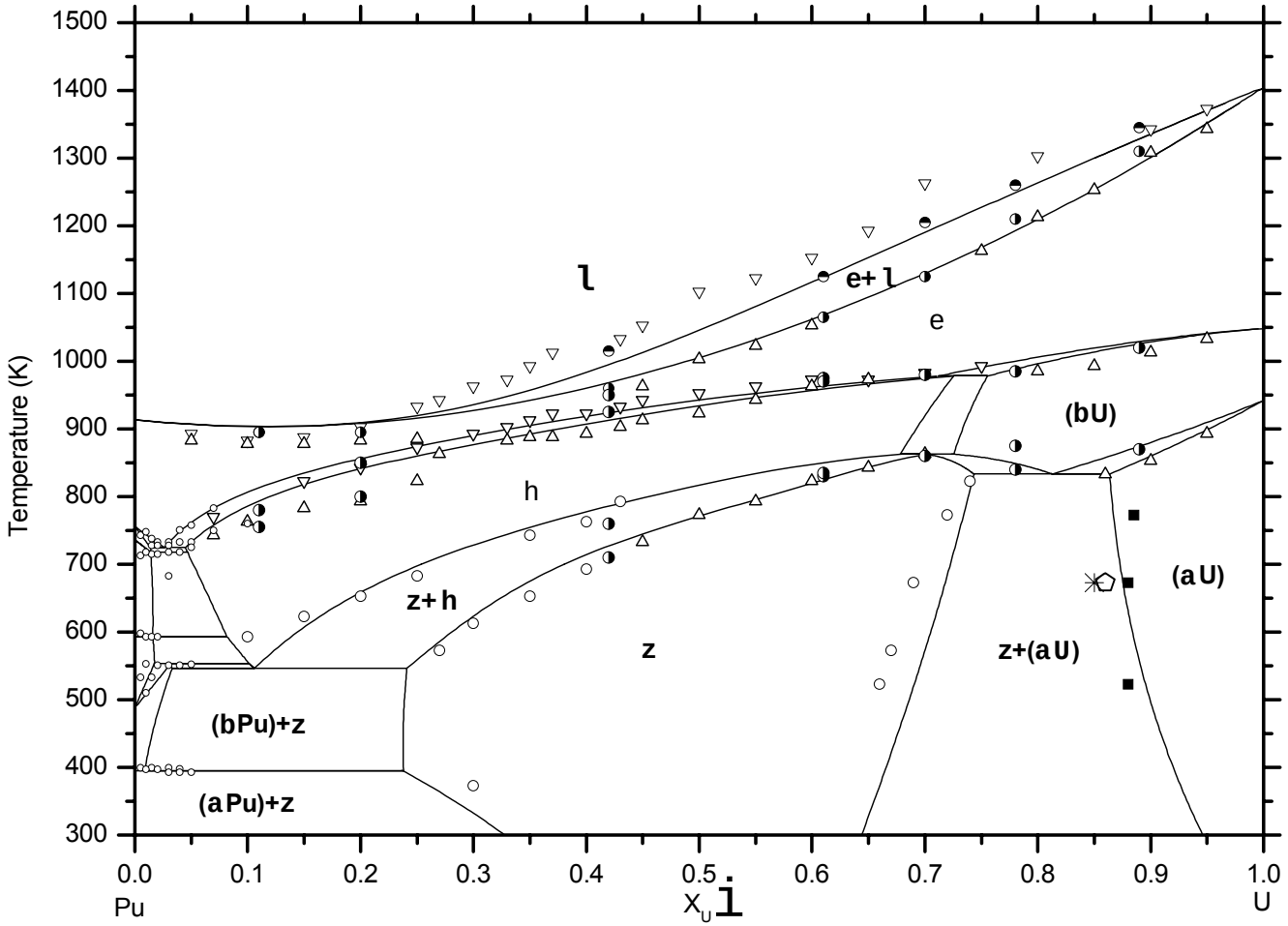

Figure 1. The plutonium-uarnium phase diagram. —— present, ▽ & △ [10], ○ Metallography [10], ○ X-ray [10], ◓ Liquidus & ◑ Solidus [17], ✳ [15], ⬠ [11]

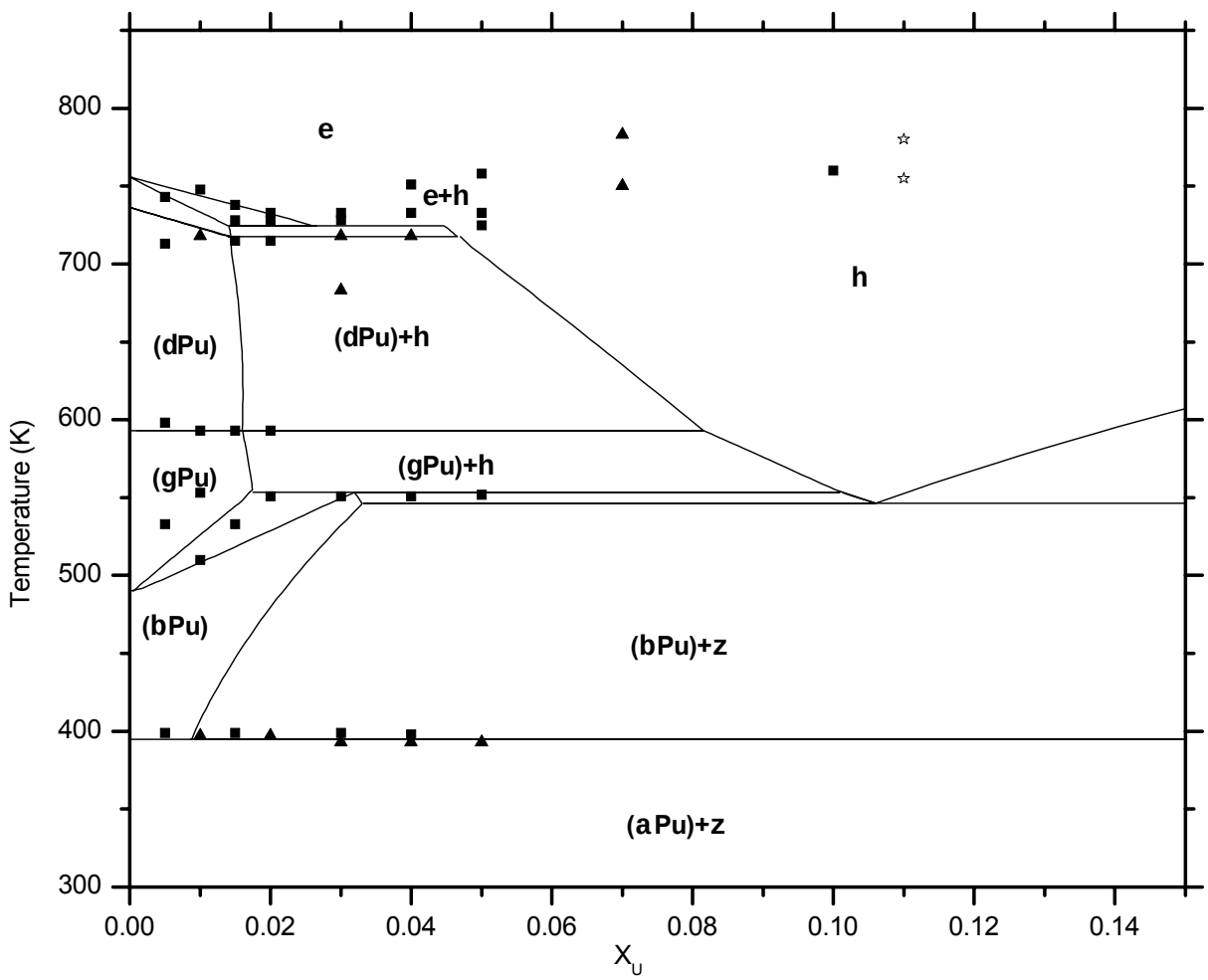

Figure 2. Plutonium rich, partial phase diagram of Pu-U binary. —— present, ▲ dilatometry [10], ■ Metallography/XRD [10], ☆ [17]

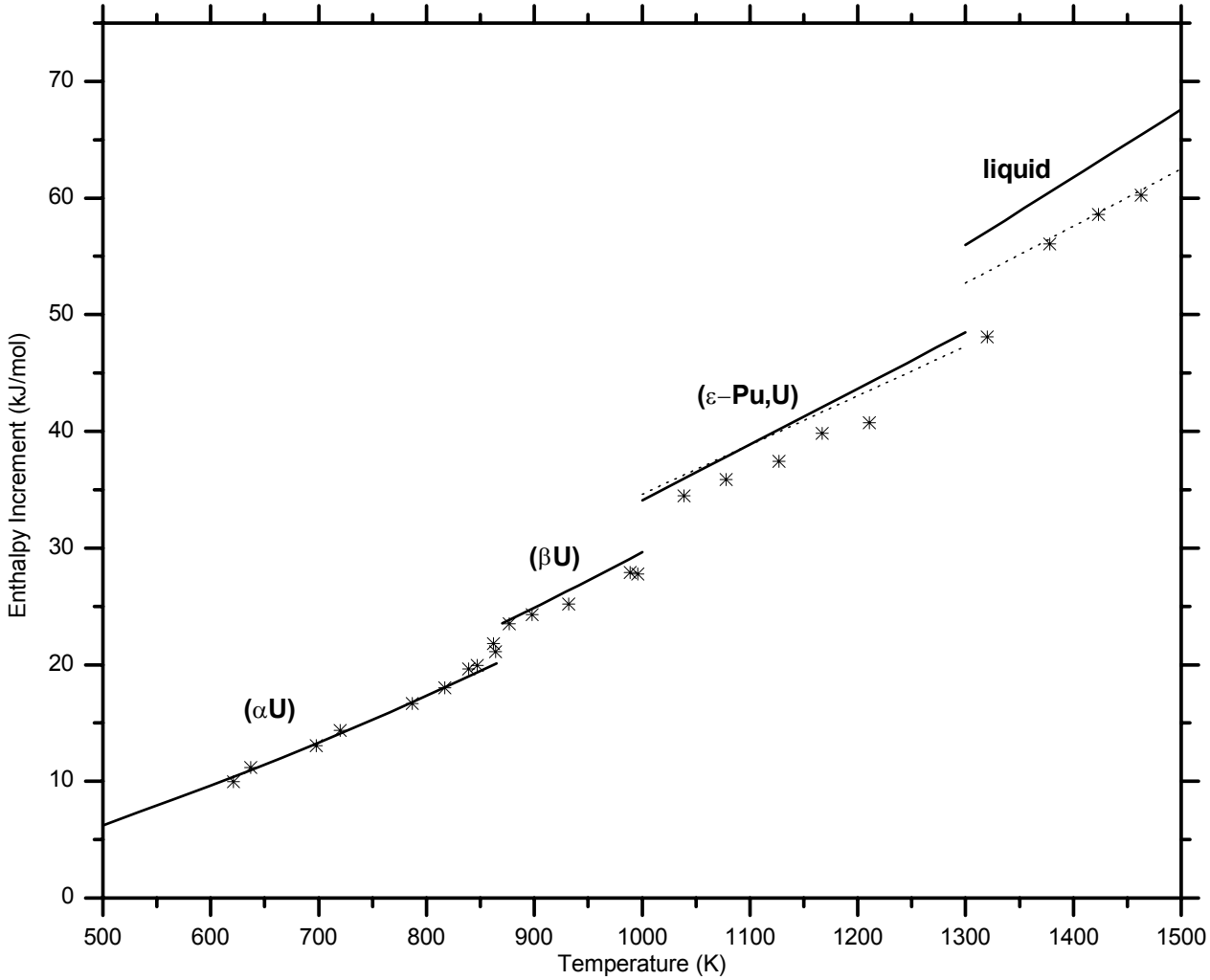

Figure 3. Enthalpy increment values of $Pu_{0.1}U_{0.9}$ alloy. ——— Present, ····· Pure Pu, ✳ Exp. [24]

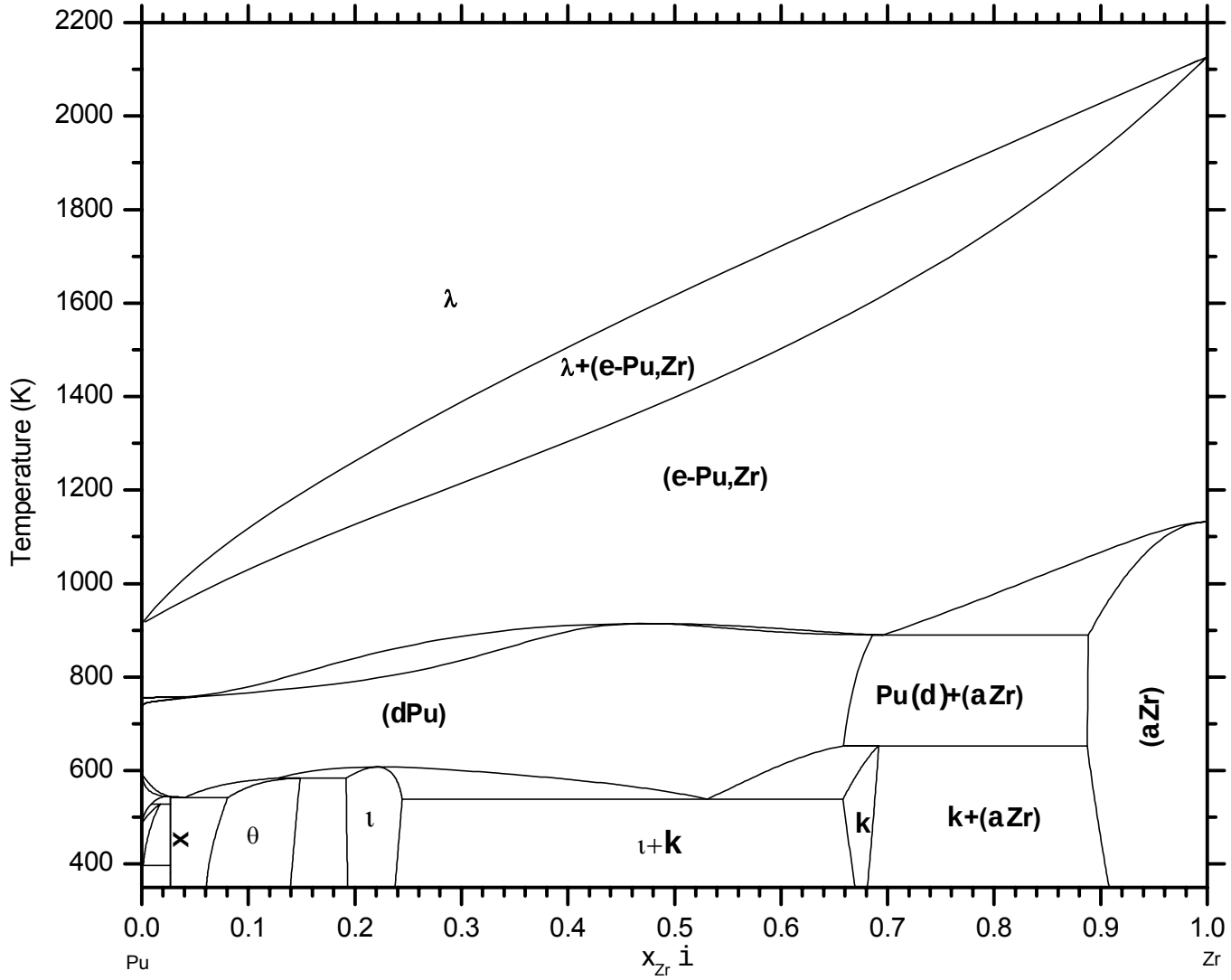

Figure 4. Calculated phase diagram of Pu-Zr binary system.

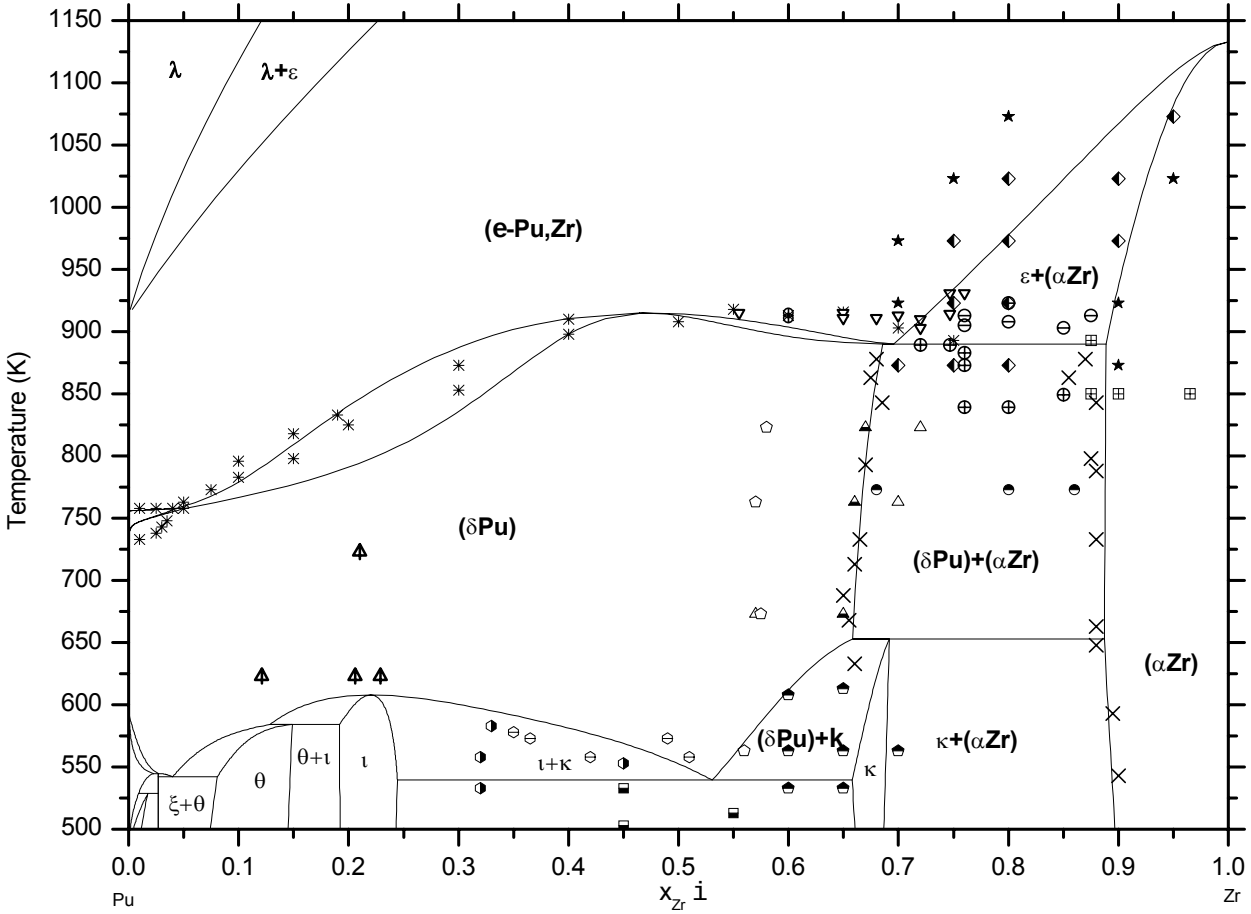

Figure 5. A comparison of calculated phase diagram of Pu-Zr binary system with experimental data.———Present, △ (dPu) [9] [28]: ✳ boundary; ◐ biphasic; ★ Single phase,[11]: ⬠ (dPu); ◓ (dPu)+k; ◑ (dPu)+Q; ⬓ Q+k; ◓ (aZr)+(dPu), [29]: × boundary, ⊖ (aZr)+e; ⊕ (dPu)+e; ⊕ (aZr)+(dPu); ⊞ (aZr); ▲ (dPu)

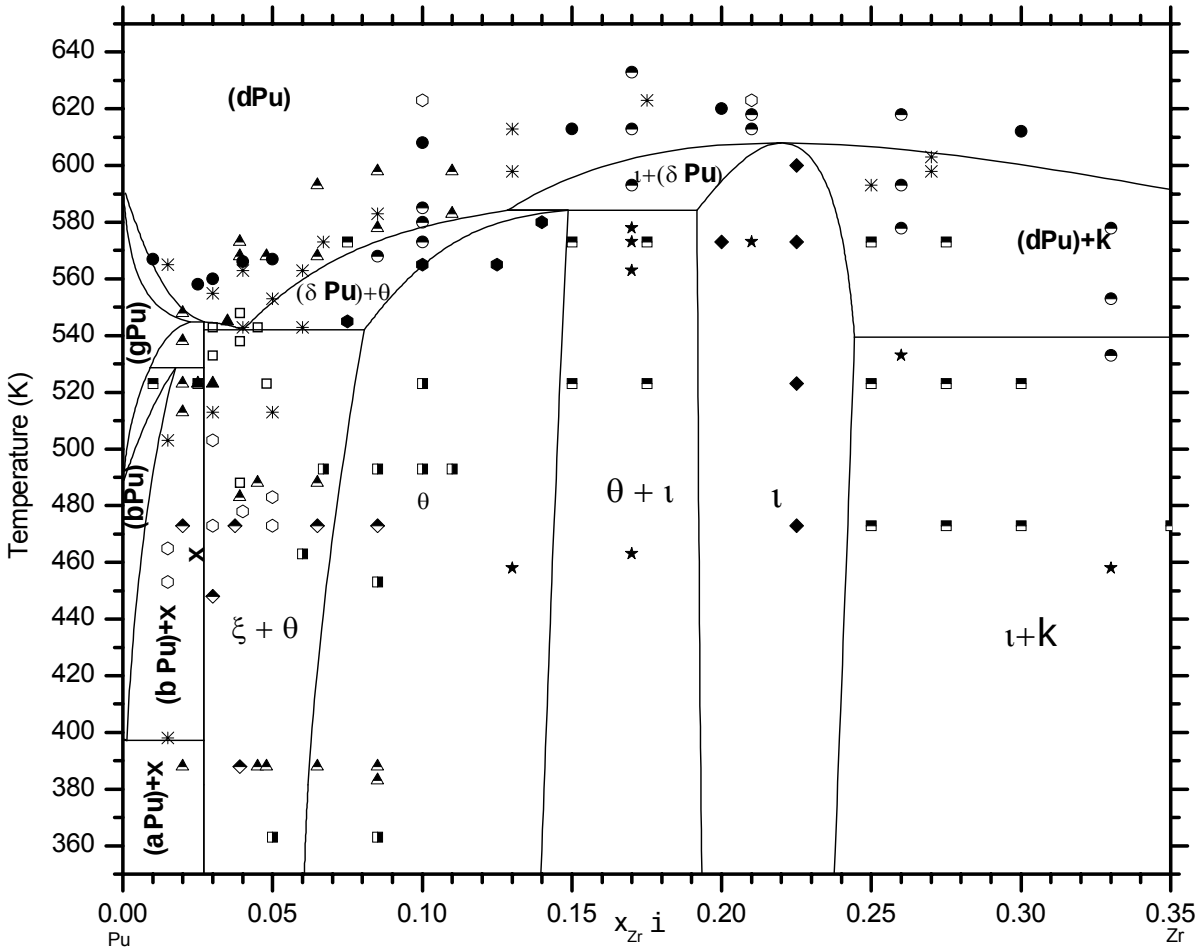

Figure 6. Plutonium rich, partial phase diagram of Pu-Zr.—— Present, [35]: ▲ (Pu)+x; ◆ (Pu)+Q; □ x, [28]: ■ biphasic; ▲ x; ● Q; ◆ i; ● (dPu), [29]: ✳ boundary; ◓ Q+(dPu); ◨ (Pu)+Q; ⬡ (Pu); ★ Q

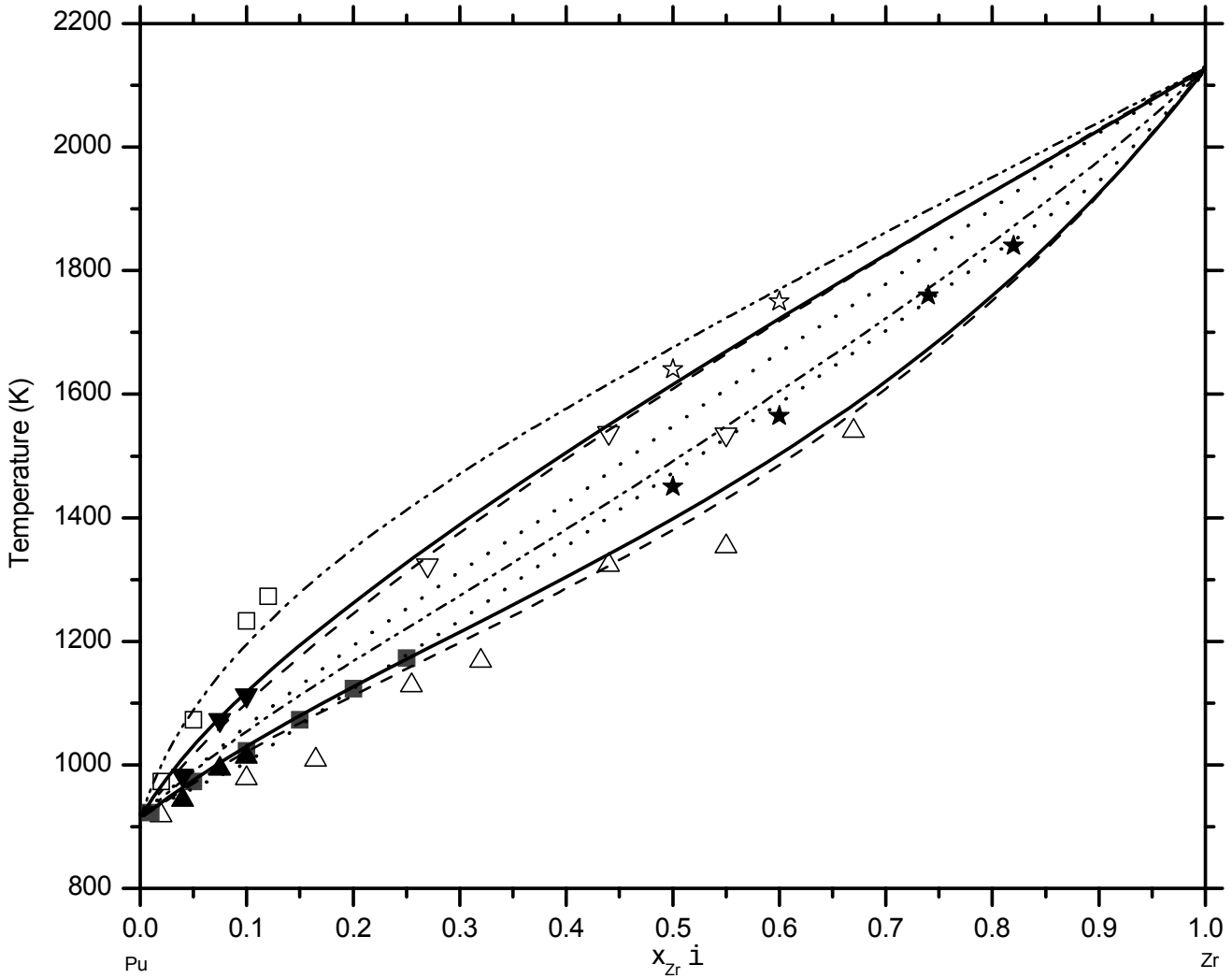

Figure 7. Liquidus-solidus of Pu-Zr.——— Present,-·-·-·- Calc.[93],– – – - Calc.[26],· · · · ·[9], (△ ,S ▽ L) [29], (■ S, □ L)[43], (▼ L, ▲ S)[31], (★ ,S ☆ L)[45]

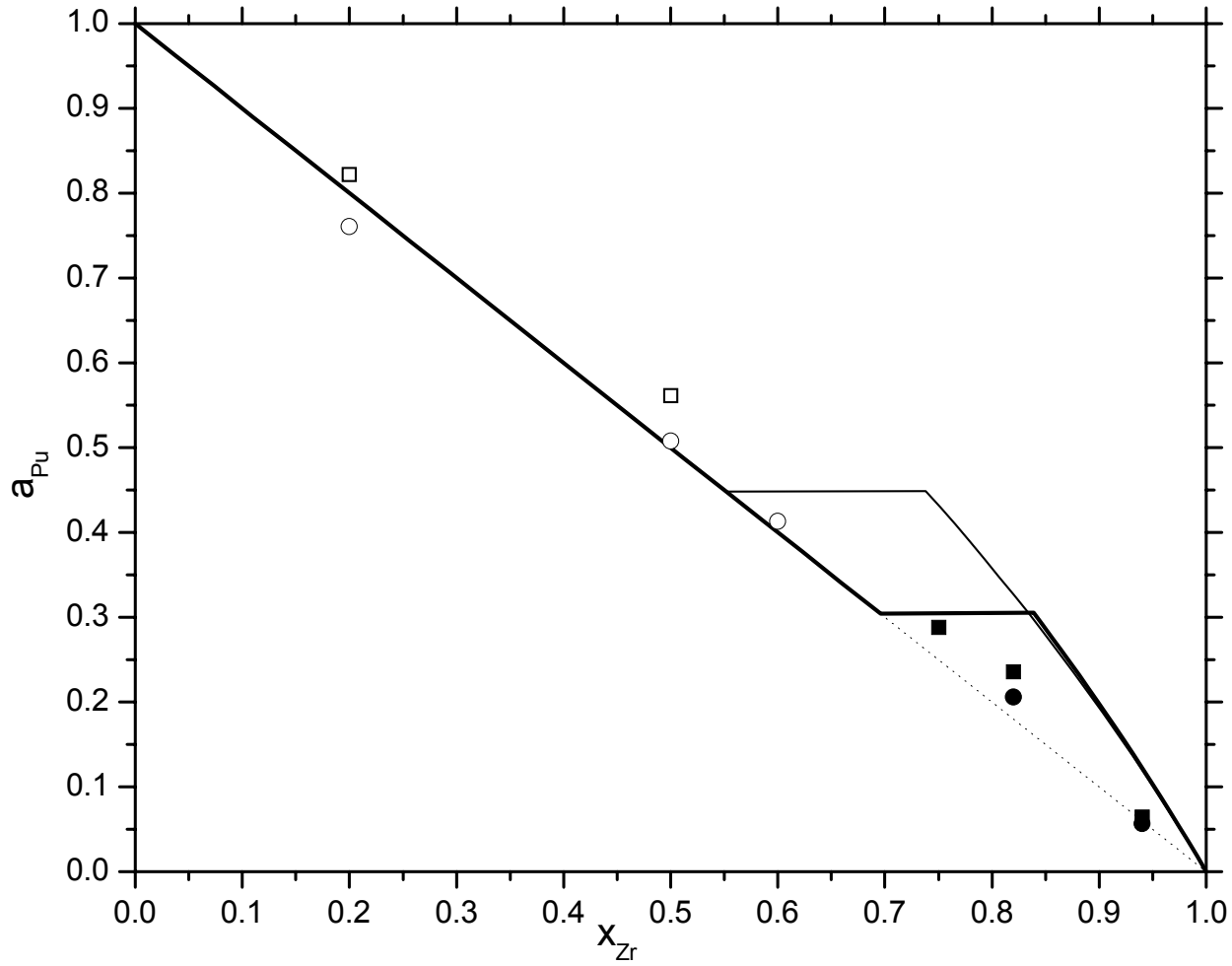

Figure 8. Activity of plutonium in Pu-Zr alloys. ——1673 K & ——1823 K (present calc. wrt Pu(l)), ····· Ideal Sol., [45]: ■ (S) 1673 K; □ (L) 1673 K; ● (S) 1823 K; ○ (L) 1823 K

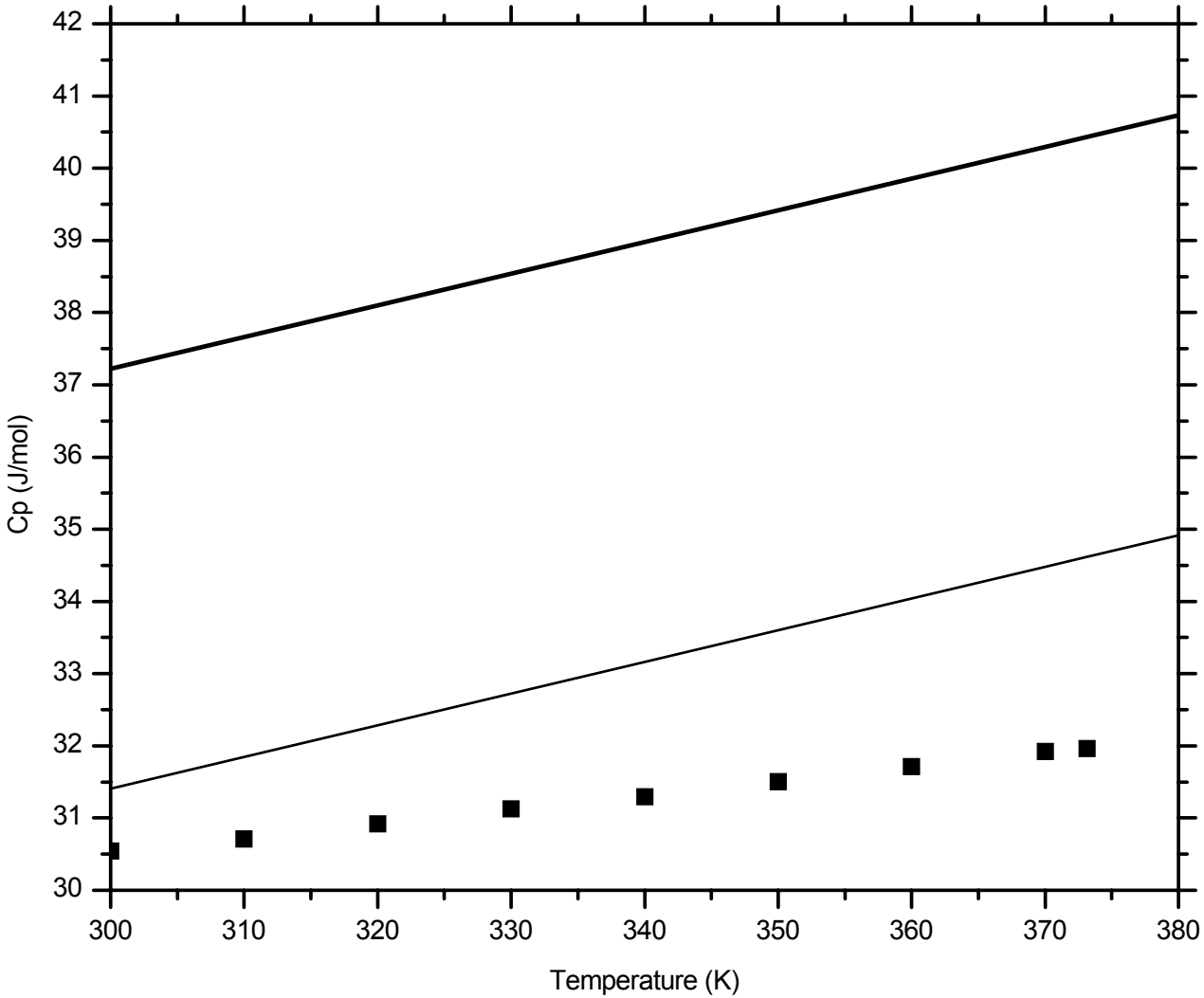

Figure 9. Heat capacity of x-compound of Pu-Zr system. ——— present, ——— Newmann-Kopp's, ■ [39]

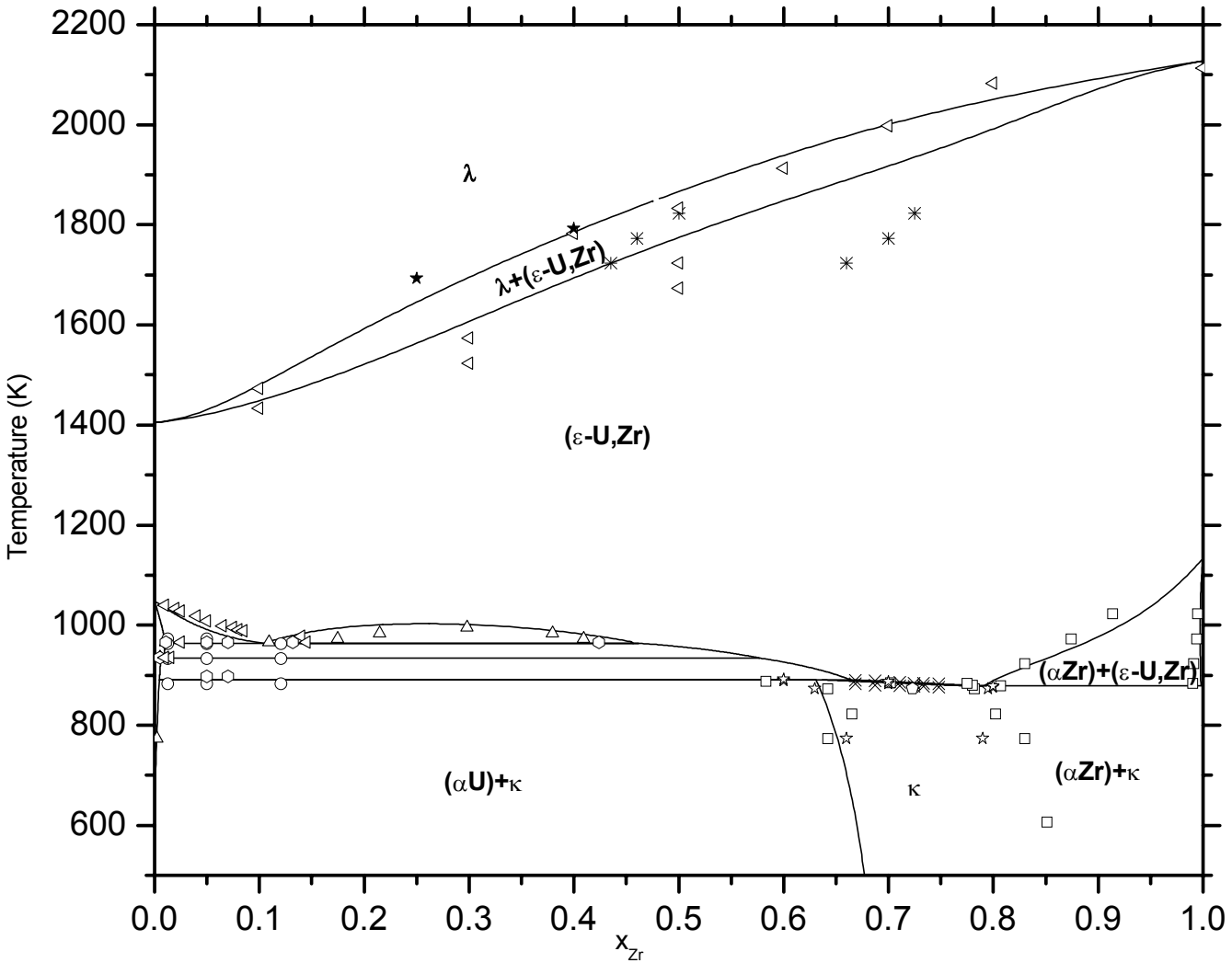

Figure 10. Phase diagram of U-Zr system.——— Present, × [65], △ [50], □ [72], ☆ [59], ⬠ [66], ◁ [49], ○ [61], ⬡ [53], ✳ [76], ★ [77]

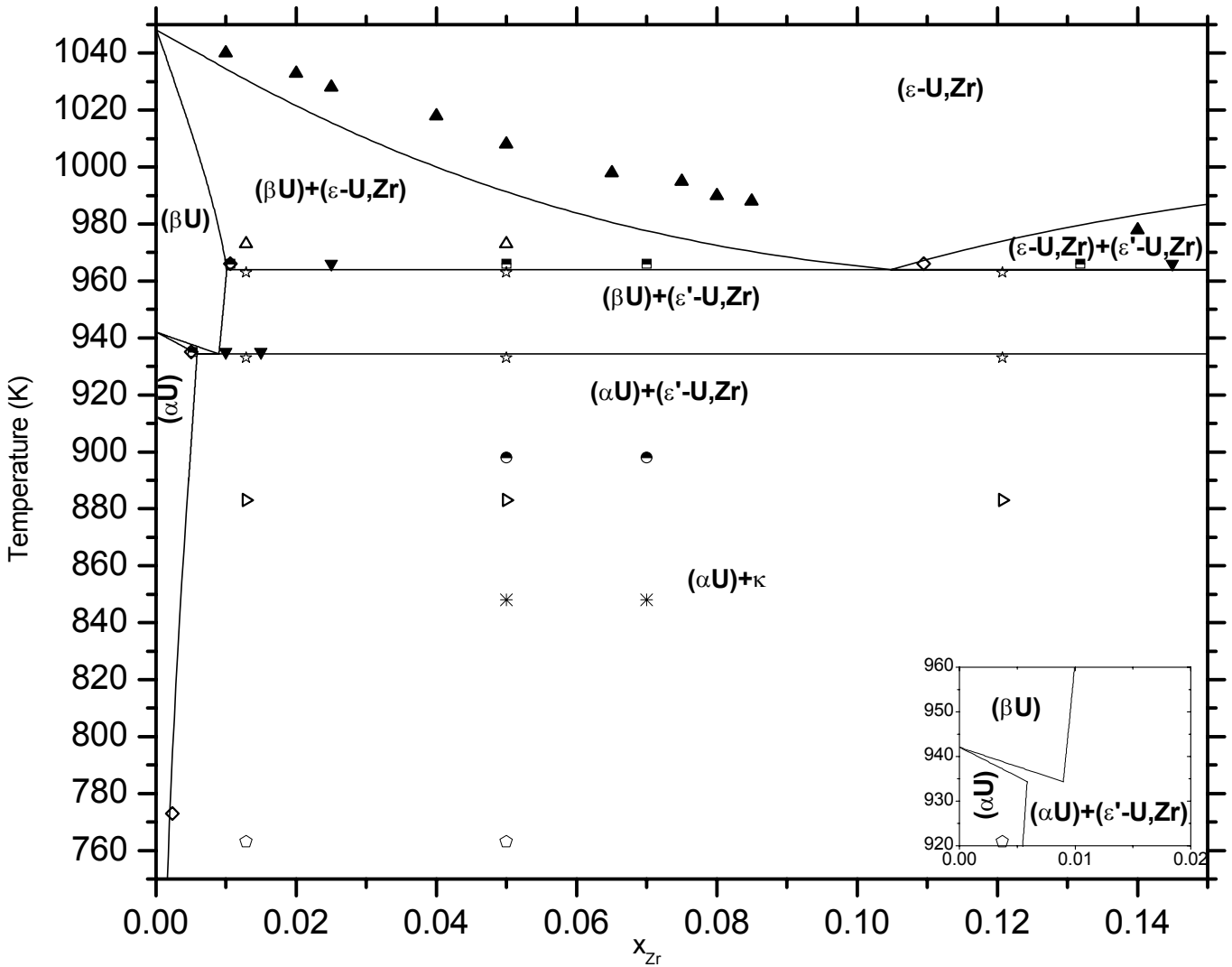

Figure 11. Uranium rich partial phase diagram of U-Zr.——— Present, (▲ & ▼) [49], ◇ [50], [61]: △ (βU)+ε; ☆ (βU)+ε'; ▷ (αU)+ε'; ⬠ (αU)+κ, [53]: ▬ Transition; ✳ (αU)+κ; ◓ (αU)+ε'

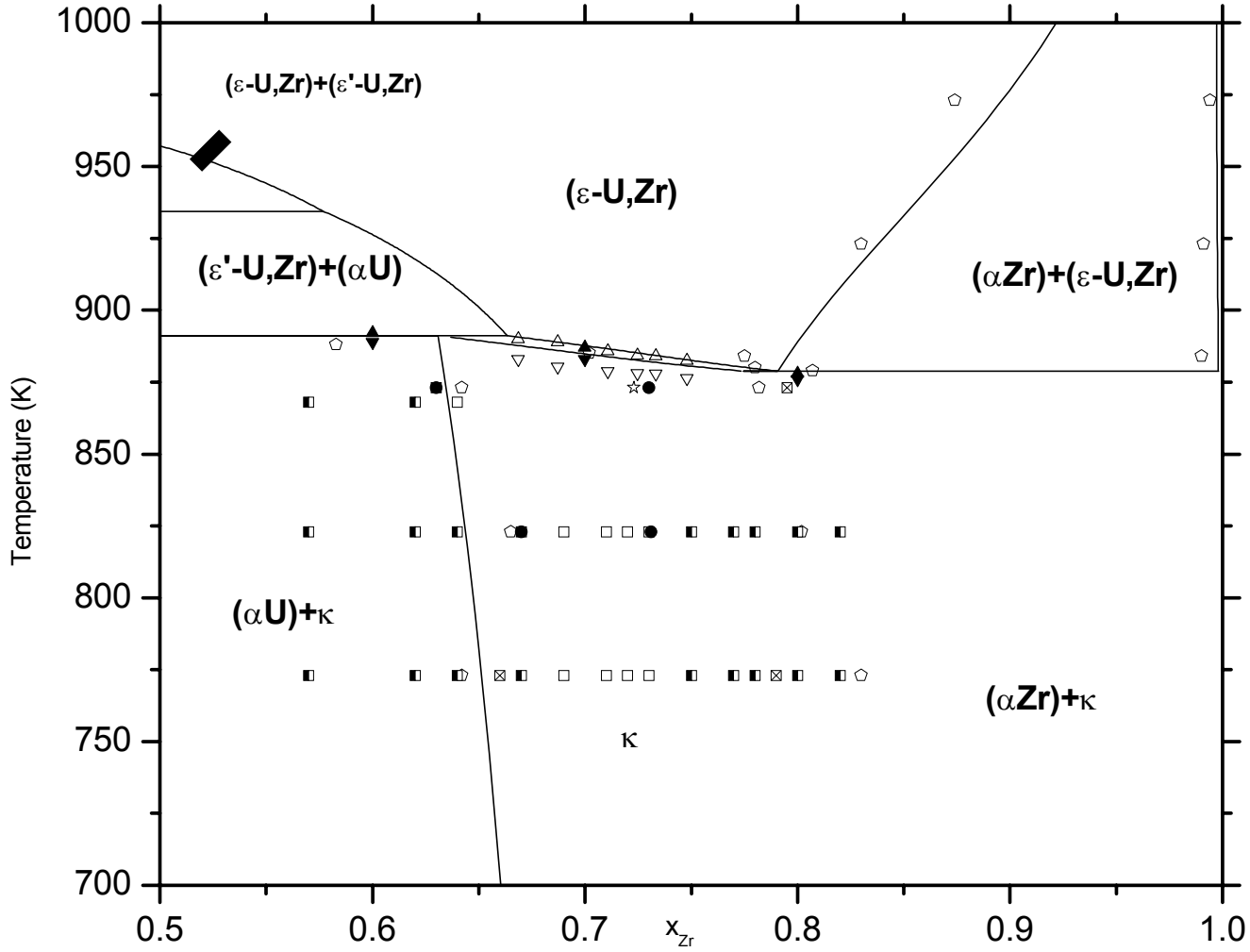

Figure 12. Zirconium rich partial phase diagram of U-Zr.——Present, ⬠ [72], ☆ [66], [59]: ⊠ κ (Metallography); (▼ & ▲)(Dilation), [65]: △ & ▽ DTA; ◧ Biphasic; □ κ (microstructure); ● κ (Hardness)

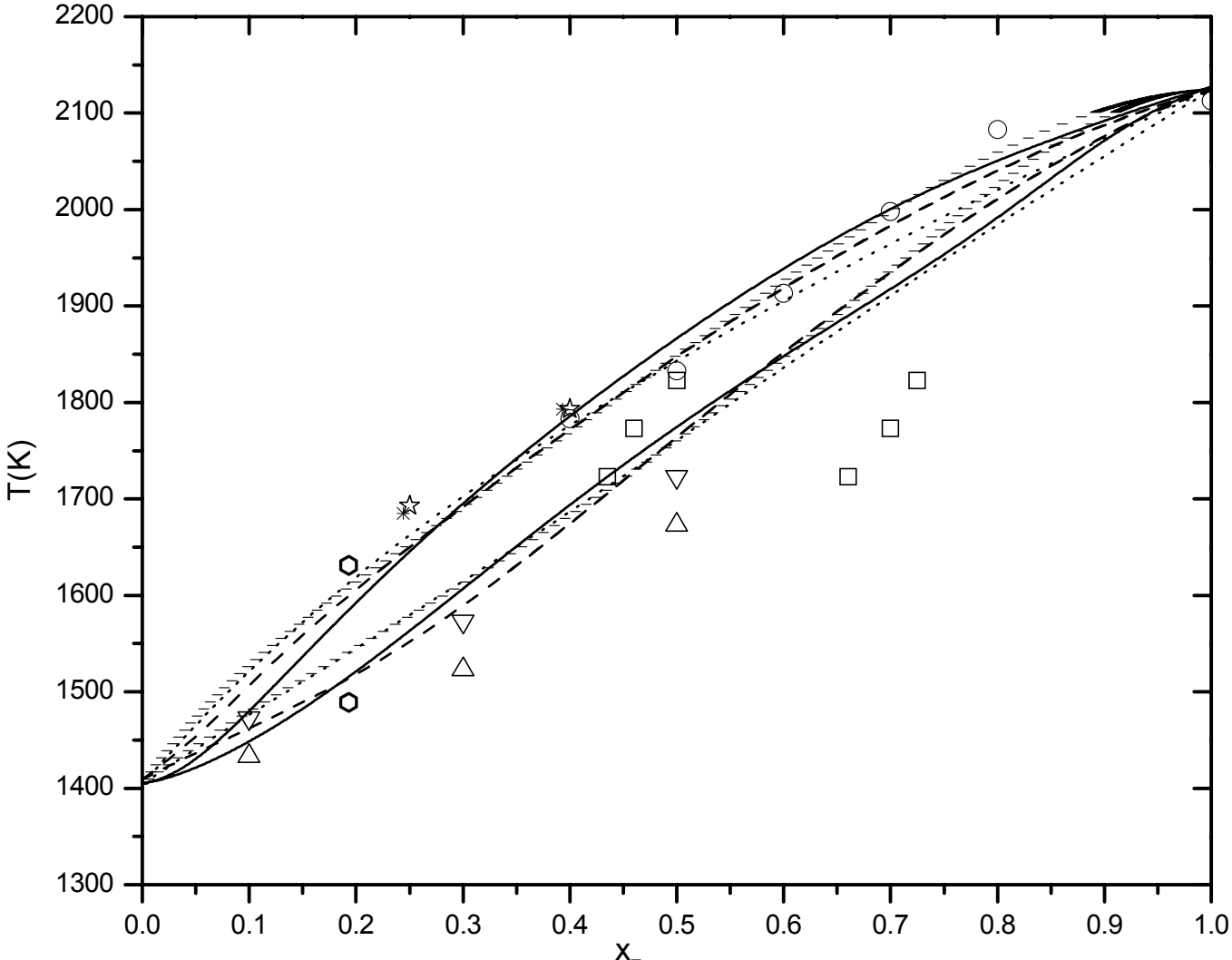

Figure 13. Liquidus-solidus of U-Zr system. —— present, – – – [82], · · · · · · [26], □ [76], (△ & ▽) [49], ○ L [49], ☆ [77], – [52], ⬡ [26], ✳ [79]

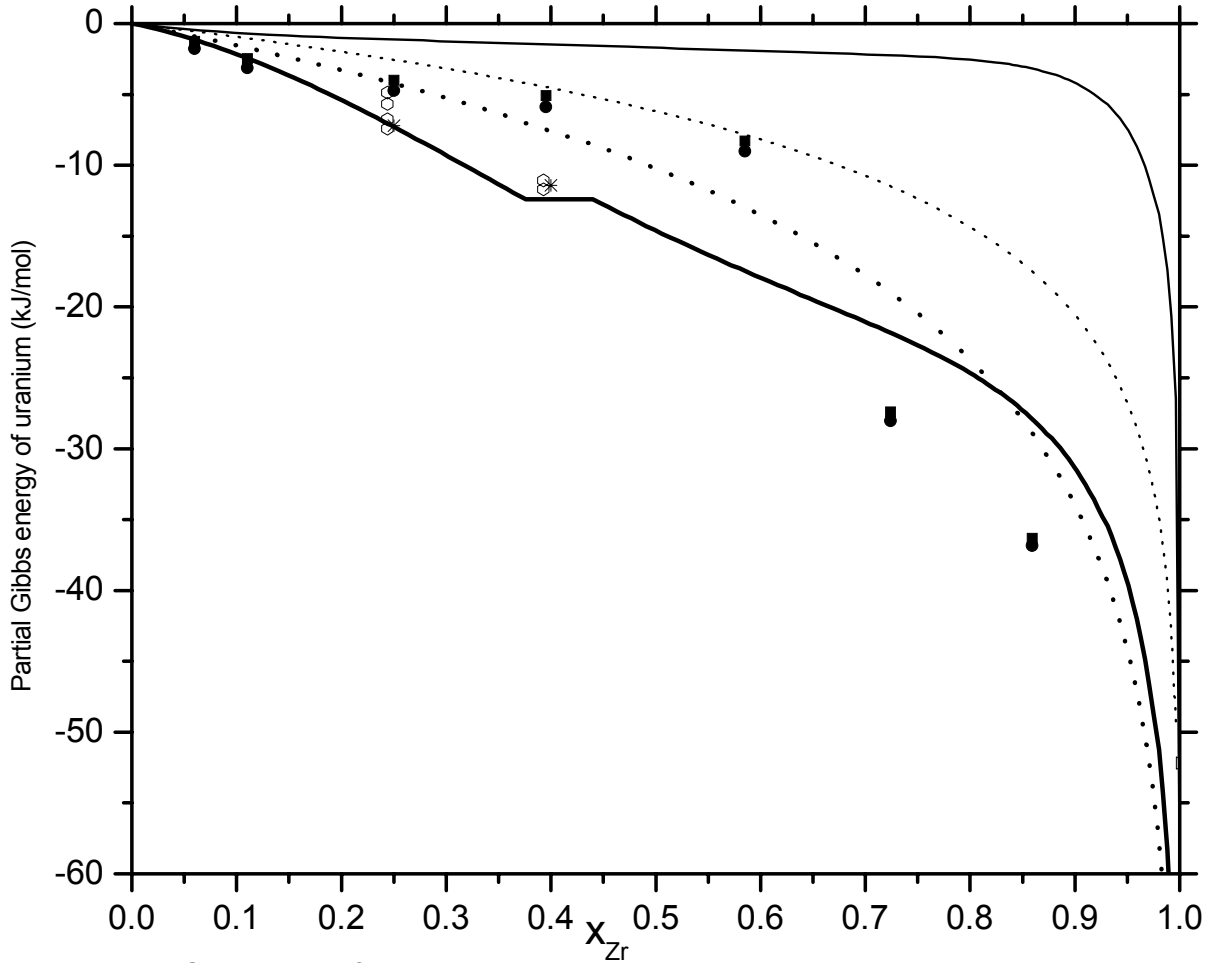

Figure 14. Partial Gibbs energy of uranium in U-Zr alloys. (——— 1773K,——— 1073K) Present, ✳ 1873K [77], ▷ 1773K [76], (· · · · · · 1073K,· · · · 1773K)Ideal, (■ 1030K, ● 1184K) [78], ⬡ (1673-1873K) [79]

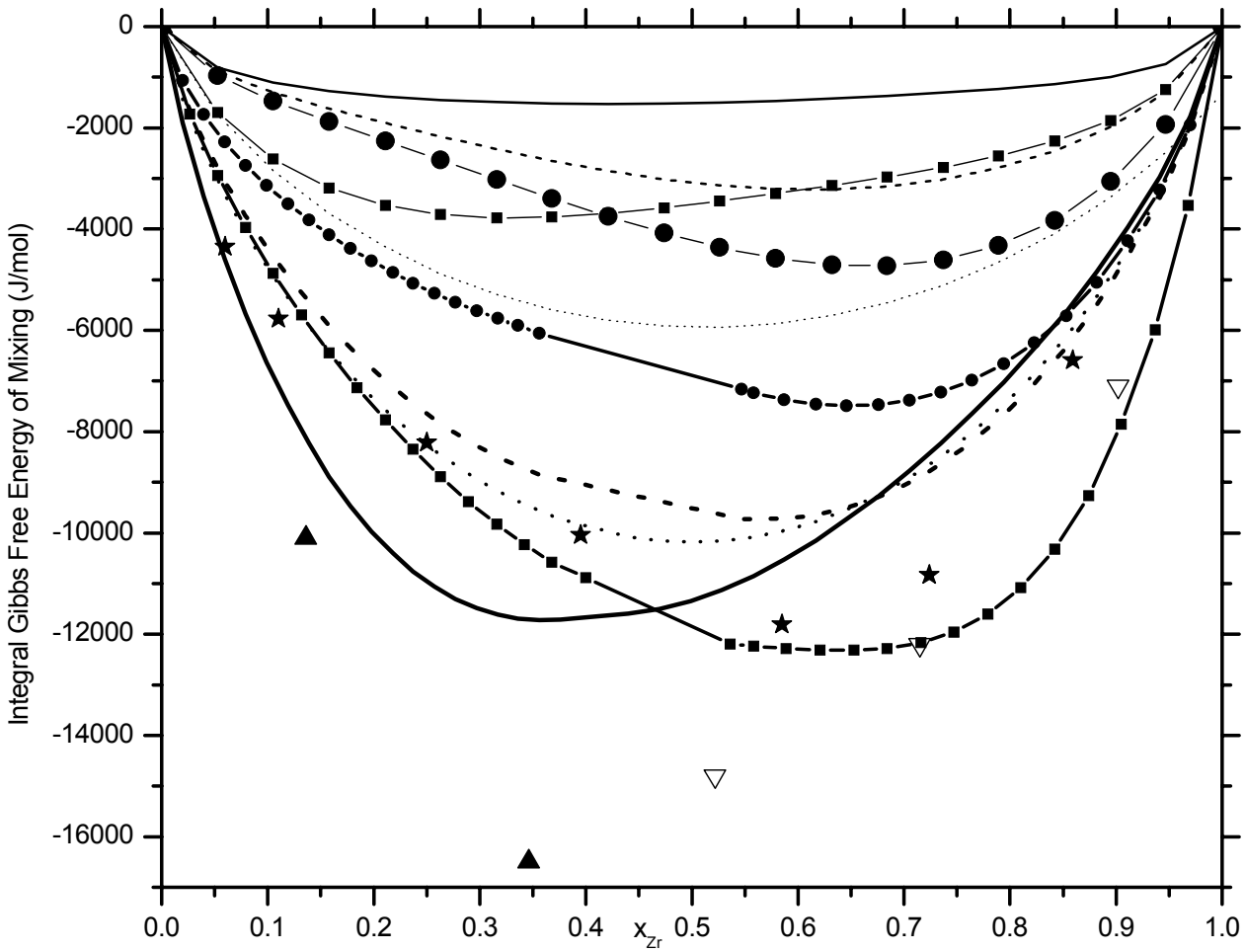

Figure 15. ΔG^{mix} of U-Zr. (——1773K,——1073K) Present, (· · · · 1773K,·····1073K) ideal,(—■—1073K,—■—1773K) [27], (—●—1073K,—●—1773K) [26], (- - - - 1073K,- - - -1773K) [82], (▽ (S), ▲ (L)) 1773K [76], ★ 1073K [78]

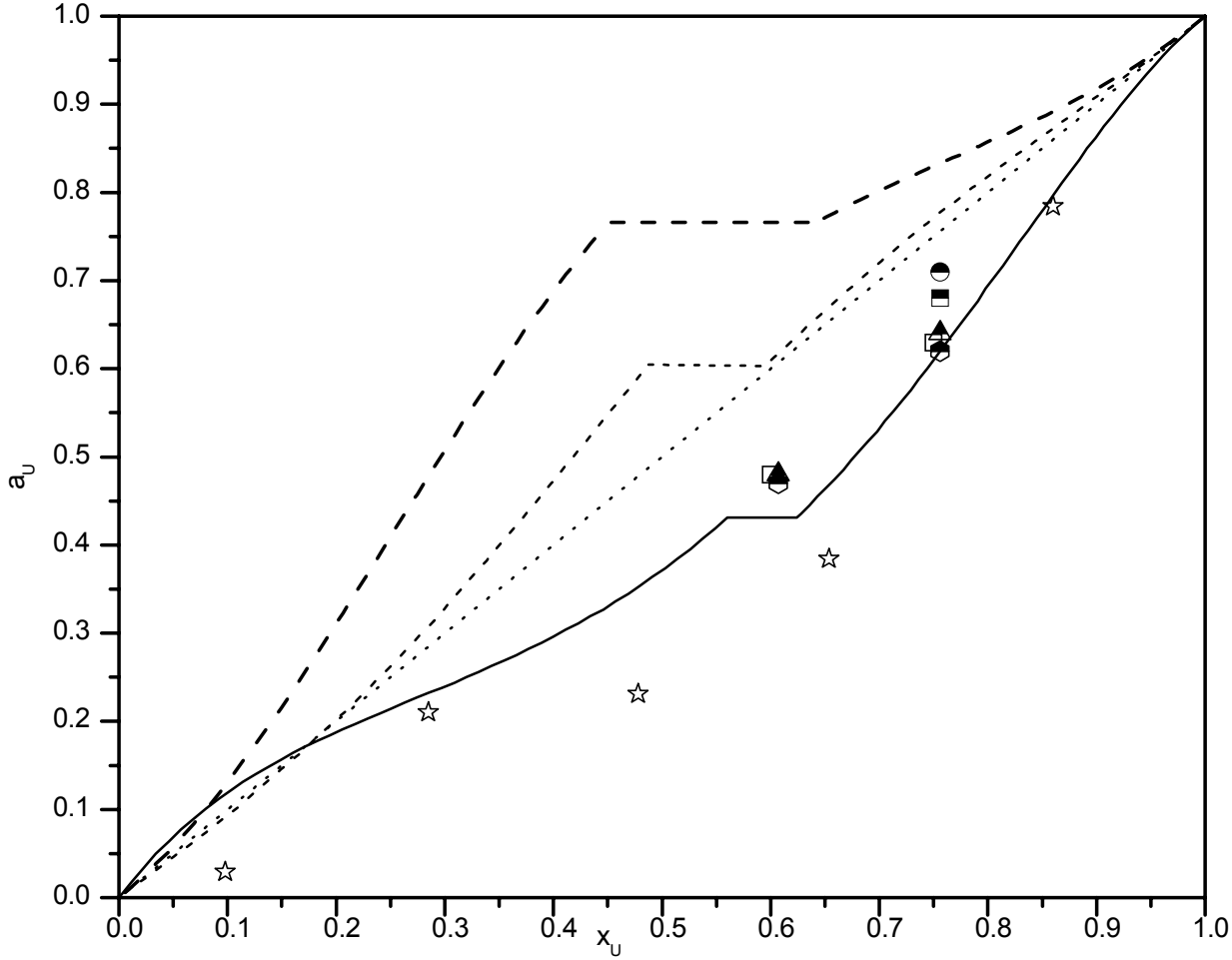

Figure 16. Activity of uranium in U-Zr. (◓ 1873K, ▲ 1823K, ◘ 1773K, ◓ 1723K) [79], ☆ 1773K [76], ——— (1773K) Present, ····· Ideal, □ 1873K [77], - - - - - 1773 K [82], – – – 1773K [26]

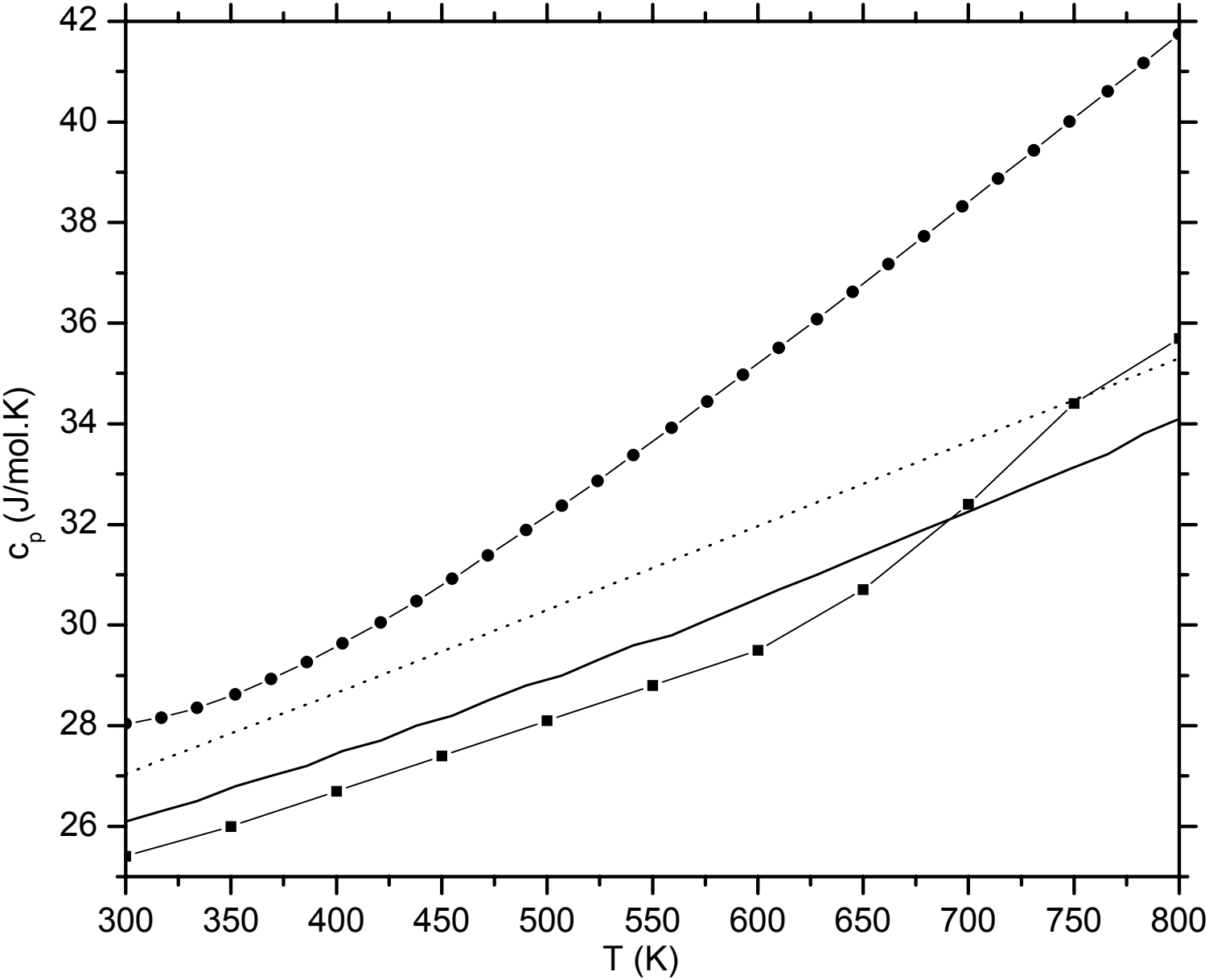

Figure 17. Heat capacity of k-UZr_2. —— present, ····· Neumann-Kopp's, —●— [63], —■— [80]

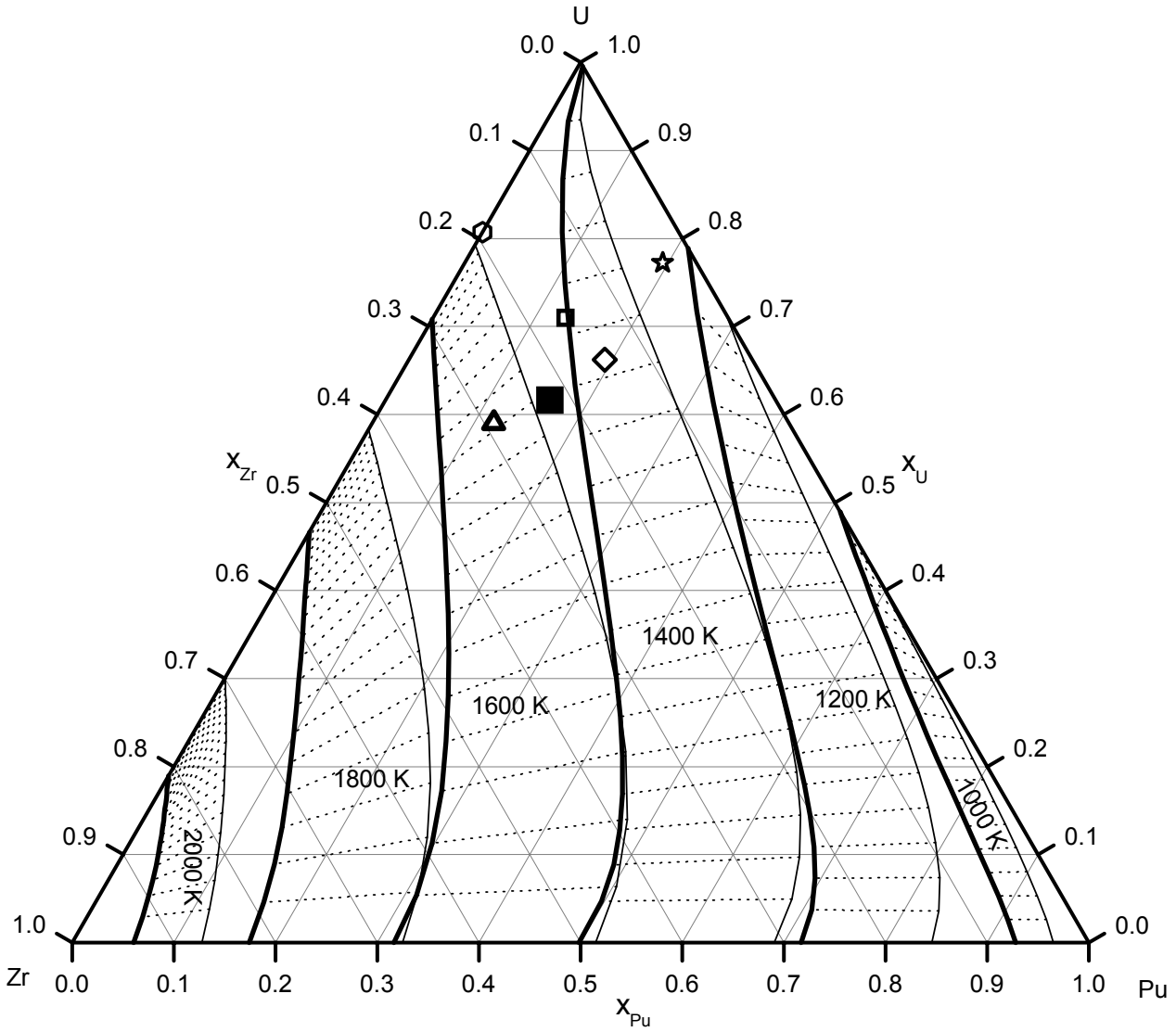

Figure 18. The calculated liquidus (———) and solidus (━━━) surfaces of Pu-U-Zr system along with tie lines (·····).

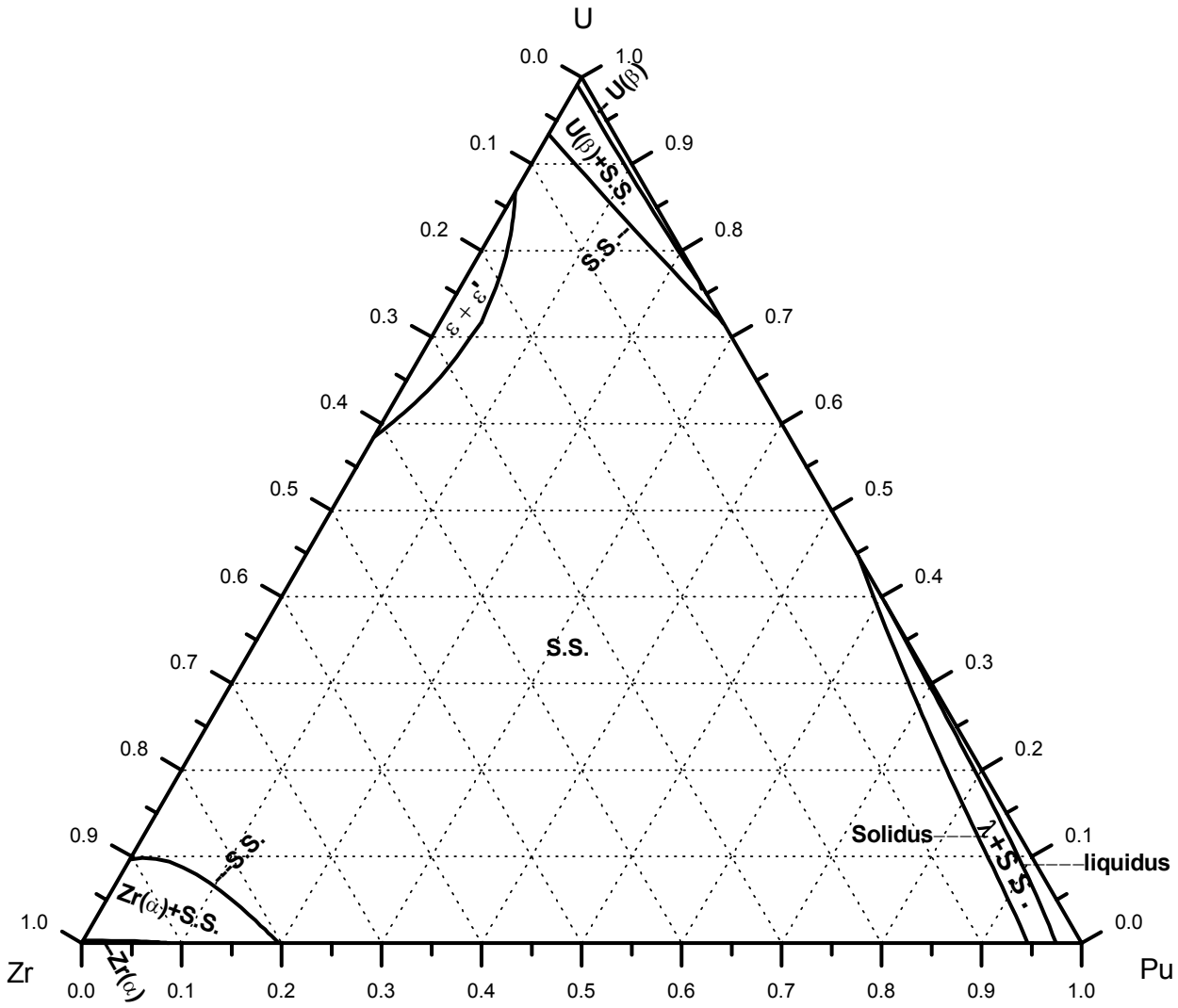

Figure 19. A calculated phase diagram of Pu-U-Zr system at 980 K.